applied sciences

MDPI

Review

Synergy of Plasma Processing and Optical Emission Spectroscopy in Food Safety Control

Sanda Pleslić [1], Eda Jovičić [1], Franka Markić [2] and Nadica Maltar-Strmečki [2,*]

[1] University of Zagreb, Faculty of Electrical Engineering and Computing, Unska 3, 10000 Zagreb, Croatia; sanda.pleslic@fer.unizg.hr (S.P.); eda.jovicic@fer.unizg.hr (E.J.)
[2] Ruđer Bošković Institute, Bijenička Cesta 54, 10000 Zagreb, Croatia; fmarkic@irb.hr
* Correspondence: nstrm@irb.hr

Featured Application

A potential application of this work is the real-time monitoring and control of plasma-assisted food processing using optical emission spectroscopy (OES). By non-invasively tracking key plasma parameters such as temperature and particle density, OES enables the precise optimisation of plasma conditions without disturbing the process. This capability supports improved quality control, including the detection of contaminants and verification of mineral composition in food products. Ultimately, integrating OES into industrial plasma systems enhances food safety, process efficiency, and the development of innovative functional foods.

Abstract

The food processing industry is seeking new technologies to enhance product safety, extend shelf life, and optimise food quality in response to growing consumer demand for high-quality products. Since the discovery of plasma technology, its potential applications in food processing have been numerous. For most of these applications, plasma characterisation is key to successfully scaling up from laboratory to industrial settings. A highly valuable tool for plasma characterisation is optical emission spectroscopy (OES), which serves as a non-invasive diagnostic method to monitor reactive species, specifically excited atoms and molecules (reactive oxygen and nitrogen species—RONS) that are critical for food treatment. The main role of OES in food control is to enable species identification and real-time process monitoring, providing feedback on electron temperature and density to prevent thermal damage to sensitive food products. It also facilitates optimisation by adjusting voltage and gas flow rates to maximise the production of antimicrobial species. These results ensure that processes are reliable and repeatable, supporting the transition from laboratory-scale to industrial applications. The paper provides an overview of the use of optical emission spectroscopy in various applications of plasma technology in food processing, including the determination of the elemental composition of raw materials and final products, detection of contaminants, quality control, determination of characteristic plasma parameters, and ensuring compliance with food safety regulations.

Keywords: optical emission spectroscopy (OES); plasma processing; plasma monitoring; plasma diagnostics; inductively coupled plasma OES (ICP-OES); microwave-induced plasma OES (MIP-OES); dielectric barrier discharge OES (DBD-OES); plasma jet OES (PJ-OES)

Academic Editors: Žydrūnas Kavaliauskas, Liutauras Marcinauskas and Viktorija Grigaitienė

Received: 9 February 2026
Revised: 26 February 2026
Accepted: 2 March 2026
Published: 4 March 2026

1. Introduction

A gas is a state of matter in which each particle, molecule, or atom moves almost independently of the others, with an average energy per particle that is very high (up to the order of 1 eV), so that intermolecular forces have a small effect on particle motion except during collisions. By adding energy to the gas and increasing its temperature, the mean energy per particle reaches the order of 10 eV, which marks the emergence of the plasma state. As a result, the mean speed of particle movement increases. In addition to elastic collisions, which also occur in ordinary gases, various inelastic processes take place, including the ionisation of gas atoms. Ionisation is a process in which, during a collision between two atoms, an electron is removed from the electron shell of one of them; for this to occur, the energy of at least one of the two atoms in the collision must be greater than the ionisation energy. For most atoms, this energy is about 10 eV, corresponding to the mean energy of the thermal motion of gas atoms at a temperature of about 116,000 K, so ionisation through inelastic collisions between atoms is also called thermal ionisation. Thermal ionisation will also occur in a neutral gas at lower temperatures than the aforementioned 100,000 K, because in the tail of the Maxwell distribution of atomic velocities, there will always be enough high-energy atoms capable of ionising another atom. Therefore, the fundamental difference between a neutral gas and plasma is the presence of particles in an ionised state, such as positive and negative ions, free radicals, electrons, and photons, as well as the presence of an electromagnetic field that fluctuates rapidly in space and time and affects the movement of charged plasma particles [1].

Plasma technology, particularly non-thermal plasma (NTP) or cold plasma (CP) technology, has been recognised as an alternative to conventional thermal technologies in food processing [2–5]. Non-thermal plasma interacts with food mainly through the generation of highly reactive oxygen and nitrogen species (ROS and RNS), which react with food surfaces, leading to oxidation, nitration, and structural changes [6,7]. It has been investigated for various applications, mainly for the microbial inactivation [8–10] and surface decontamination [11–13] of food products, with the aim of improving food safety [14–16] and extending shelf life [17–19].

Despite its promising potential, cold plasma remains a relatively underexplored technology in food processing, and many aspects of its interaction with food matrices are not yet fully understood. The impact of cold plasma treatment depends on several factors, including plasma generation conditions, gas composition, treatment time, and the characteristics of the treated food [20–22]. Therefore, there is a growing need to develop reliable and standardised methods to evaluate the effects of cold plasma on food products and to accurately characterise the plasma itself [23]. These approaches are important for better understanding and controlling processing parameters, improving the reproducibility of results, and supporting the further application of cold plasma technology in the food industry.

Due to the complex composition and dynamic behaviour of plasma systems, reliable diagnostics such as plasma spectroscopy [24] are required to characterise and monitor properties for the optimisation of food processing. Among the radiative processes in plasma, line radiation corresponds to transitions of electrons between different levels in ions and atoms, and at lower temperatures, in molecules. The emission of radiation at discrete frequencies, i.e., wavelengths, is a quantum-mechanical phenomenon in which electrons move from one energy level to another, emitting photons whose energy is exactly equal to the difference between the energies of the initial and final states (Figure 1) [1].

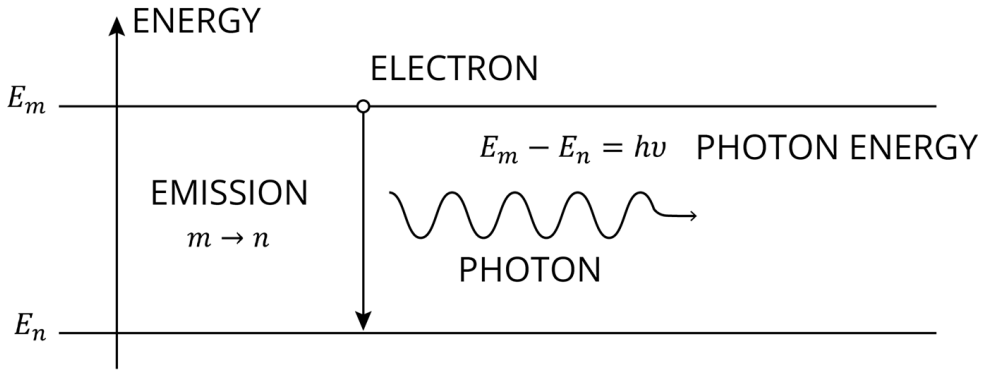

Figure 1. Scheme of atom energy levels with two energy states.

Optical emission spectroscopy (OES) is a key analytical technique based on measuring electromagnetic radiation emitted from excited ions, atoms, or molecules. An optical emission spectrometer collects plasma radiation using transfer optics (lenses, mirrors, optical fibres), spectral dispersion using a high-resolution diffraction grating or prism, and light detectors (photomultipliers, photodiodes, or CCDs), which measure the intensity of light at each wavelength [25,26]. The spectrometer is connected to a computer, which receives raw OES data (a set of wavelength–intensity pairs over the entire wavelength range of the spectrometer). After data processing, the results are clearly displayed in real time on a computer monitor as an emission spectrum. Experimental measurements can be stored for further calculations or simply printed. The user interface ensures minimal operator intervention; the only requirement is to set the spectroscopic measurement parameters initially (such as data update rate, integration time, and number of scans to average). The principle of OES operation is shown schematically in Figure 2. Each chemical element emits light at unique frequencies or wavelengths, allowing qualitative identification. The intensity of the emitted radiation is proportional to the concentration of the element in the sample, enabling quantitative analysis. OES is recognised as a highly selective and sensitive analytical technique [27–29].

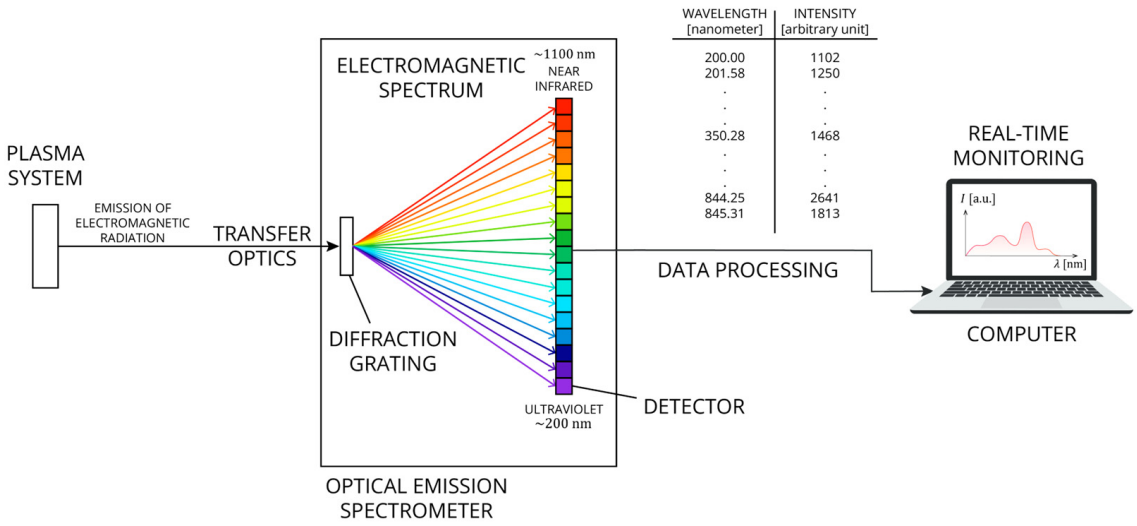

Figure 2. Schematic representation of optical emission spectroscopy (OES).

Typical optical emission spectroscopy encompasses a wide spectral range to include all necessary spectral lines for complete sample analysis: from the ultraviolet (UV) region of the electromagnetic spectrum (200–380 nm), which is crucial for detecting elements such as boron (B), carbon (C), phosphorus (P), and sulphur (S); through the visible region

(380–750 nm), used for analysing many metals such as aluminium (Al), copper (Cu), and iron (Fe); to the near-infrared (NIR) range (750–1100 nm), which enables the detection of elements such as oxygen (O) and nitrogen (N) in some materials [26,30].

The synergy between plasma processing and OES in food safety involves using OES as a real-time, non-invasive sensor to monitor and control non-thermal plasma (NTP) treatments, ensuring efficient microbial inactivation while preserving food quality, including nutrients, flavour, and texture. OES analyses the excited species in plasma, providing crucial data on electron temperature and density, which enables the precise adjustment of plasma parameters such as voltage, frequency, and gas flow to optimise decontamination and prevent unwanted chemical changes. This supports effective food safety control and industrial scale-up [31–33].

This review presents an overview of the combined application of plasma technology and optical emission spectroscopy in the food industry, highlighting the role of OES in plasma characterisation and in evaluating plasma–food interactions. Particular attention is given to the use of OES for determining key plasma parameters and process monitoring, as well as its role in applications related to food safety, quality control, and regulatory compliance.

2. Inductively Coupled Plasma–Optical Emission Spectroscopy (ICP-OES)

Inductively coupled plasma (ICP) is generated in a system comprising a radio frequency (RF) power source, a cylindrical reactor chamber with a coil, and a gas unit (Figure 3). The sample is nebulised and introduced into a flow of plasma carrier gas, usually argon. The RF generator produces an oscillating current in an induction coil wrapped around the tube. The induction coil creates an oscillating magnetic field, which induces an oscillating current in the ions and electrons of the carrier gas. These ions and electrons transfer energy to other atoms in the working gas through inelastic collisions, ionising them and forming plasma. The plasma excites the atoms in the nebulised sample, causing them to emit radiation at wavelengths characteristic of each element. The emitted light is measured by an optical emission spectrometer (OES), which enables the simultaneous detection and quantification of up to 70 elements, as the radiation intensity is proportional to concentration. The intensity of each spectral line is then compared to previously measured intensities of known element concentrations, and the concentrations are calculated by interpolation along calibration lines [31,34,35].

Due to its high sensitivity, accuracy, and ability to simultaneously measure multiple elements, inductively coupled plasma optical emission spectroscopy (ICP-OES) has been widely applied in numerous studies to evaluate the elemental composition of foods [36], providing valuable data for food safety, nutritional assessment, and regulatory purposes.

It is an ideal method for both routine and advanced analysis, enabling the processing of various types of samples after appropriate preparation [37], rapid and efficient analysis of large numbers of samples, and supporting quality control [38], authenticity [39,40], and food safety assessments [41]. In many cases, dietary regulations for essential elements cannot be established because of a lack of analytical data on their content in locally available foods. Consequently, ICP-OES has been used in research to provide reliable data on essential elements in locally consumed foods.

2.1. Nutritional Elements in Food Products

ICP-OES has been extensively applied to determine essential minerals in staple foods, providing valuable information for dietary intake assessments and nutritional evaluation. For example, manganese was quantified in 89 food items purchased randomly from major markets and hypermarkets, digested by wet ashing and prepared for analysis under properly adjusted operating conditions (power, wavelength 257.610 nm, plasma flow, etc.)

in Egypt [42], showing that fat-rich foods (6.75 µg/g), nuts (4.64 µg/g), and protein-rich foods (4.52 µg/g) contained the highest Mn levels, while meat had the lowest (0.53 µg/g). These data illustrate how elemental composition can vary significantly depending on food type, soil composition, and processing.

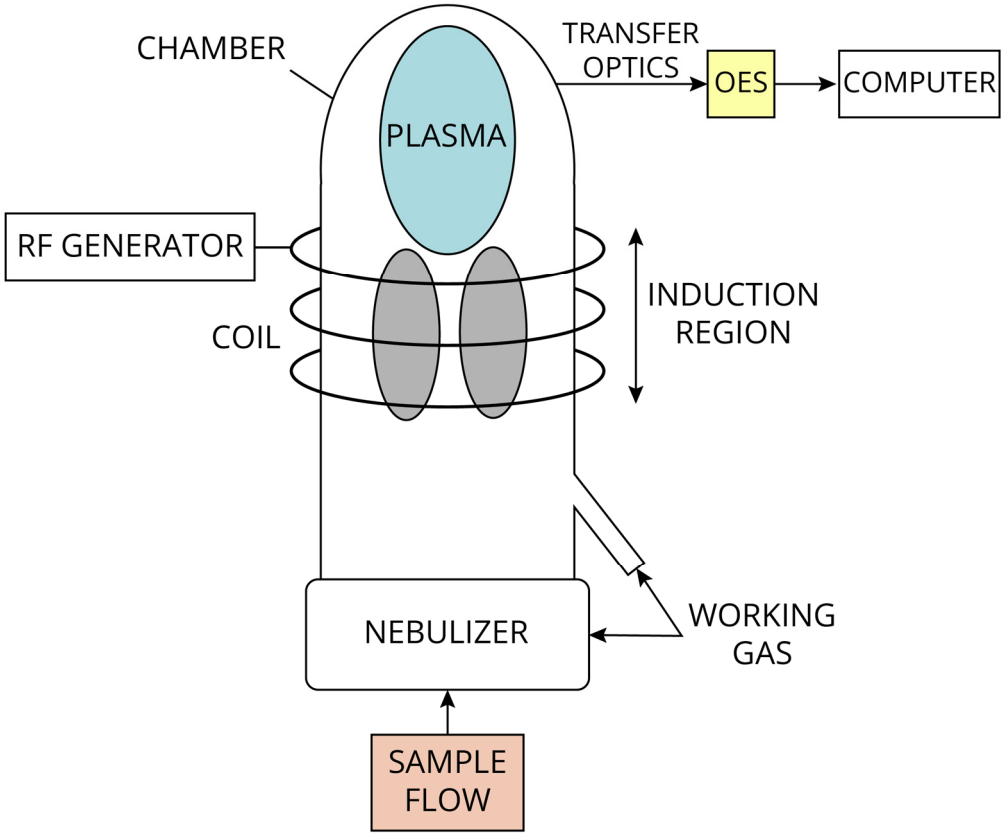

Figure 3. Schematic of inductively coupled plasma–optical emission spectroscopy (ICP-OES).

In another study [43], the daily intake of macro-elements (Na, K, Ca, Mg) and trace elements (Cr, Se) from the main food groups (cereals, milk products, potatoes, vegetables, fruits, eggs, fish, meat, fats and oils, sweets, water, and drinks) was assessed in young adults. The selective parameters of the applied spectroscopic determinations were, among others, LOD—limit of detection and LOQ—limit of quantification in µg/kg for Cr (1.2 and 4.3) and Se (2.2 and 7.5). Daily Cr intake was 148 ± 7 µg/kg for women and 177 ± 5.36 µg/kg for men, while Se intake was 106 ± 8 µg/kg for women and 119 ± 7.70 µg/kg for men. These results highlighted the main food groups contributing to total intake and showed that some individuals consumed levels above the recommended reference values (Cr for women 25 µg/kg, for men 35 µg/kg; Se for women and men 45 µg/kg).

Plant-based foods are also important sources of essential minerals. Pseudocereals such as quinoa, amaranth, and buckwheat provide Cu, Mn, Fe, Zn, Mg, Ca, P, Na, and K, making them valuable for gluten-free and vegetarian diets. ICP-OES has been used to determine their mineral content accurately [44]. In addition, three digestion procedures were previously performed, dry ashing, microwave, and graphite block acid digestion, to find the optimal digestion method. Emission lines were chosen for selected elements, LOD and LOQ values in mg/kg were reported for each element and each type of digestion. Although the microwave method of digestion proved to be optimal, it was recommended, if possible, to compare the results of ICP-OES for all three digestion procedures to confirm the nutritional contribution of minerals and to support dietary recommendations.

Legumes, including Phaseolus, Vicia, Pisum, and Lathyrus species, are an important source of macro- and micro-elements, such as K, Ca, Mg, P, Fe, Zn, Cu, and Mn. The integrated approach in [45] first involved microwave-assisted acid digestion followed by ICP-OES. Multiple elements were tested including macro-elements (P at 213.617 nm; K at 766.490 nm; Ca at 317.933 nm; Mg at 285.213 nm), micro-elements (Fe at 238.204 nm; Cu at 327.393 nm; Zn at 206.200 nm; Mn at 257.610 nm) and trace elements (Cd at 228.802 nm; Pb at 220.353 nm; Ni at 231.604 nm; Cr at 267.716 nm). Analysis of 38 legume samples grown in Serbia showed that among the macro-elements, K was the most abundant (8981–14,177 mg/kg), while high levels of Zn (206–238 mg/kg) and Fe (238 mg/kg) were found among the micro-elements. Trace elements such as Ni (24–57 mg/kg), Cr (0.8–4.1 mg/kg), Pb (0.07–1.2 mg/kg), and Cd (0–0.07 mg/kg) were also measured, with Pb and Cd exceeding regulatory limits in several samples. These results demonstrate the value of ICP-OES for assessing both the nutritional benefits and safety of legumes, and supporting dietary evaluation and food quality monitoring.

ICP-OES is a reliable analytical tool for determining nutritional elements in food products, as it provides accurate and reproducible data important for routine analyses (Table 1).

Table 1. ICP-OES technique: nutritional elements in food products.

Sample	Determination	Reference
89 food items randomly purchased from the main markets and hypermarkets in Alexandria Governorate	Mn	[42]
Cereals, milk and dairy, potatoes, vegetables, fruits, eggs, fish, meat and meat products, fats and oils, sweets and sugars, water and beverages	Cr, Se	[43]
Pseudocereals: quinoa, amaranth, buckwheat	Cu, Mn, Fe, Zn, Mg, Ca, P, Na, K	[44]
Legumes—4 different species (*Phaseolus* spp., *Vicia* spp., *Pisum* spp. and *Lathyrus* spp.)	P, K, Ca, Mg, Fe, Cu, Zn, Mn, Cd, Pb, Ni, Cr, As	[45]

2.2. Food Safety and Toxic Elements

ICP-OES has been widely applied to assess the presence of toxic elements in food, providing critical information for public health and regulatory compliance. A study [46] evaluated the risk of heavy metal exposure (Cd, Pb, Hg, and Ni) from various food categories, including meat, fish, eggs, dairy, vegetables, fruits, cereals, oils, sweets, beverages, and water. The results showed that daily intake of Cd, Hg, and Ni was well below the limits set by the European Food Safety Authority (EFSA), while Pb intake posed a potential health risk, highlighting the need for continuous monitoring.

Many types of honey are sold on the Greek and global markets without indicating the levels of certain toxic metals. In research [47], 25 minerals (Ag, Al, As, B, Ba, Be, Ca, Cd, Co, Cr, Cu, Fe, Hg, Mg, Mn, Mo, Ni, Pb, Sb, Se, Si, Ti, Tl, V, Zn) were quantified in several types of Greek honey, including asfaka, fir, flower, forest flower, and orange blossom honeys. Lead concentrations in many samples exceeded the recommended limit of 0.10 mg/kg, reaching up to 0.47 mg/kg in flower honey from Samos Island, indicating the importance of monitoring heavy metals in food production and improving quality control measures.

Spices, used globally for culinary, pharmaceutical, and cosmetic purposes, are another food group where the metal content is relevant. In a study [48], 17 elements, including essential micronutrients (Cr, Mn, Fe, Co, Zn) and toxic metals (Pb, Cd), were analysed in 22 commonly consumed spices (asteroid anise, clove, cardamom, cinnamon, coriander, turmeric, cumin, white pepper, black pepper, nutmeg, allspice, chilli, paprika, ginger, green pepper, pink pepper, and curry) from the Greek market. The ICP-OES method was shown to be rapid and simple, and was validated in terms of precision, limit of detection (LOD) and limit of quantification (LOQ). Good linearity was achieved for all analytes, and the

LOD and LOQ values were 0.08–5.95 mg/kg and 0.27–19.83 mg/kg, respectively. The following emission lines were selected for identification: 328.068 nm (Ag), 308.215 nm (Al), 249.772 nm (B), 230.425 nm (Ba), 223.061 nm (Bi), 317.933 nm (Ca), 226.502 nm (Cd), 238.892 nm (Co), 357.869 nm (Cr), 324.752 nm (Cu), 238.204 nm (Fe), 280.271 nm (Mg), 257.610 nm (Mn), 232.003 nm (Ni), 217.000 nm (Pb), 276.787 nm (Tl) and 213.857 nm (Zn). While essential minerals were detected at varying levels, the presence of toxic metals underscores the need for regular safety assessment of these widely consumed products.

ICP-OES is proving to be a widely applicable and reliable analytical technique for food safety and toxic element control. The simultaneous and rapid quantification of multiple elements in various food matrices distinguishes ICP-OES from other techniques used to ensure food quality and safety in compliance with regulations (Table 2).

Table 2. ICP-OES technique: food safety and toxic elements.

Sample	Determination	Reference
Cereals, milk and dairy, potatoes, vegetables, fruits, eggs, fish, meat and meat products, fats and oils, sweets and sugars, water and beverages	Cd, Pb, Hg, Ni	[46]
Asfaka, fir, flower, forest flowers and orange blossom honeys harvested in the wider area of Hellas	Ag, Al, As, B, Ba, Be, Ca, Cd, Co, Cr, Cu, Fe, Hg, Mg, Mn, Mo, Ni, Pb, Sb, Se, Si, Ti, Tl, V, Zn	[47]
Spices: asteroid anise, clove, cardamon, cinnamon, coriander, turmeric, cumin, white pepper, black pepper, nutmeg, allspice, chilli, paprika, ginger, green pepper, pink pepper, curry	Ag, Al, B, Ba, Bi, Ca, Cd, Co, Cr, Cu, Fe, Mg, Mn, Ni, Pb, Tl, Zn	[48]

2.3. Food Authenticity and Quality Control

In recent years, ensuring food authenticity and quality has become an important research focus, particularly for high-value food products. ICP-OES has been widely applied to evaluate elemental profiles that can serve as authenticity markers. In a study of 13 Italian wine samples [49], six elements (K, Na, Mg, Ca, Rb, and Fe) were quantified using ICP-OES. Potassium was the most abundant element in all samples, with concentrations ranging from 488.7 to 1174.0 mg/L, while the levels of the other elements were consistent with data reported in the literature, confirming the authenticity and quality of the wines analysed.

The concentrations of Ni and Zn in Zambian honey collected from different regions, as detected by ICP-OES [50], remained below the permissible limits set by the World Health Organization, except for Pb concentrations from two provinces (1.10 ± 0.12 and 0.54 ± 0.02). However, public health risk assessment indicators, including estimated daily intake, target hazard quotient, and hazard index, indicated that there is no significant health risk and that Zambian honey is safe for consumption. Continuous monitoring is recommended to ensure the desired quality and authenticity.

ICP-OES has also proven effective for detecting food adulteration when combined with chemometric tools. In one study [51], the mineral composition of 73 samples of green banana flour, including both authentic and adulterated products, was analysed after microwave digestion. The wavelengths determined for monitoring were Ca (422.673 nm), K (766.490 nm), Mg (280.270 nm), Na (589.592 nm), P (214.914 nm), B (249.678 nm), Cu (327.396 nm), Fe (238.204 nm) and Mn (259.373 nm). Elements such as B, Ca, Cu, Fe, Mn, P, K, Mg, and Na were quantified, and potassium was identified as a key marker for differentiating authentic from adulterated samples. These results demonstrate the potential of ICP-OES-based elemental profiling as a simple and reliable approach for authenticity assessment in emerging food markets.

Additionally, mineral composition has been investigated as an authenticity marker for spices. In a study focused on cinnamon samples commercialised in Brazil [52], ICP-OES

was used to determine the concentrations of 12 elements following microwave-assisted acid digestion. The LOD, LOQ and wavelengths were determined for each of the 12 elements: P (213.618 nm); S (182.034 nm); Mg (280.270 nm); Ca (422.673 nm); K (766.490 nm); Cu (324.754 nm); Zn (213.856 nm); B (249.773 nm); Fe (259.940 nm); Al (396.152 nm); Mn (257.610 nm); and Si (251.611 nm). The results showed that trace element profiles could be used to distinguish Cinnamomum zeylanicum from other cinnamon species, highlighting the applicability of ICP-OES for authenticity control in plant-derived food products.

Overall, these studies show that ICP-OES can be effectively used in food authenticity assessment and quality control through the analysis of characteristic elemental composition (Table 3).

Table 3. ICP-OES technique: food authenticity and quality control.

Sample	Determination	Reference
Italian wine	K, Na, Mg, Ca, Rb, Fe	[49]
Zambian honey	Pb, Ni, Zn	[50]
Banana flour	B, Ca, Cu, Fe, Mn, P, K, Mg, Na	[51]
56 ground cinnamon samples	P, S, Mg, Ca, K, Cu, Zn, B, Fe, Al, Mn, Si	[52]

2.4. Limitations of ICP-OES: Solutions and Future Developments

The main limitations of ICP-OES relate to highly defined detection limits compared to other methods used for the same purpose, such as inductively coupled plasma mass spectrometry (ICP-MS) [53,54]; reduced reliability when processing samples with complex matrices; and the overlapping spectral lines of different elements (for example, Fe at 259.940 nm and Mn at 259.372 nm) or molecular species, which reduces accuracy [55]. In low-resolution systems, these emission lines may merge, distorting quantification unless correction is applied. Emission lines from the excited working gas near the detection limit can add noise to the signal. The optimal selection of emission lines is based on sensitivity, the minimisation or absence of spectral interference, and the detector response. Some elements have thousands of emission lines in a certain part of the spectrum, so precise wavelength selection followed by background correction is important (e.g., 259.940 nm for Fe). Commonly used analytical lines in ICP-OES for some elements with a typical range of LOD are shown in Table 4 [32,35,56].

Table 4. Representative emission lines for some elements in ICP-OES technique.

Element	Wavelength (nm)	LOD Range (µg/L or ppb)
Aluminium (Al)	396.152	0.5–2
Arsenic (As)	193.696	2–10
Calcium (Ca)	315.887/317.933	1–50
Cadmium (Cd)	214.440/228.802	0.1–1
Copper (Cu)	324.754	0.5–5
Iron (Fe)	259.940	1–10
Lead (Pb)	220.353/217.0	1–5
Magnesium (Mg)	279.078/285.213	0.1–10
Manganese (Mn)	257.610	0.1–2
Phosphorus (P)	178.222/213.618	5–20
Potassium (K)	766.491	10–100
Sodium (Na)	589.592	10–50
Zinc (Zn)	213.857	0.5–5

Sample preparation is demanding, and better results are obtained for liquid samples than for solid samples, which require digestion. End users expect lower costs and simple

application, but addressing issues related to spectral interference, matrix effects, and wavelength selection requires expertise in plasma spectroscopy.

New generations of detectors used in optical emission spectrometers have increased spectral resolution (10–20 pm in standard systems and less than 5 pm in high-resolution systems), accelerated the simultaneous analysis of several elements, and enabled greater flexibility in the choice of analyte wavelengths. The different positioning of the transfer optics relative to the plasma (radial or axial) allows for the collection of light from a larger area of the plasma, thereby increasing the instrument's sensitivity. Although ICP-MS is better for identifying and quantifying trace elements, modern axial ICP-OES is excellent at detecting trace metals in food, most often well below maximum permitted limits. The instrument size has been reduced, increasing mobility. By optimising operating conditions (gas flow, RF power, treatment time), the cost of application is reduced.

3. Microwave-Induced Plasma–Optical Emission Spectroscopy (MIP-OES)

Microwave plasma is generated by high-frequency electromagnetic waves using a method based on a magnetron rather than electrodes. A magnetron is an electron tube consisting of a cathode surrounded by a cylindrical anode. Electrons emitted by the cathode move towards the anode under the influence of a magnetic field and, as they pass the resonant cavities inside the anode, transfer part of their energy to the high-frequency field in the resonators, thereby sustaining the oscillation. The magnetron serves as a signal source in the gigahertz range. The microwaves delivered by the waveguide accelerate gas electrons during collisions, inducing ionisation and the subsequent emission of photons in the UV and visible regions of the spectrum, which can be effectively monitored by OES (Figure 4). Adjusting the gas flow and viewing position (height, radial position) in microwave-induced plasma optical emission spectroscopy (MIP-OES) optimises sensitivity and minimises matrix effects; higher flow rates often improve detection limits, while viewing deeper in the plasma or along the axis enhances the signal for certain elements. The method offers the advantages of producing stable, energetic plasma at atmospheric pressure with low operating costs, high electron density, efficient generation of reactive oxygen and nitrogen species (RONS), and electrodeless operation, which eliminates the risk of contamination. Owing to these advantages, MIP-OES is used as an advanced analytical method for multi-element analysis of a wide range of complex samples, such as biomaterials and food, and for quality control [2,57,58].

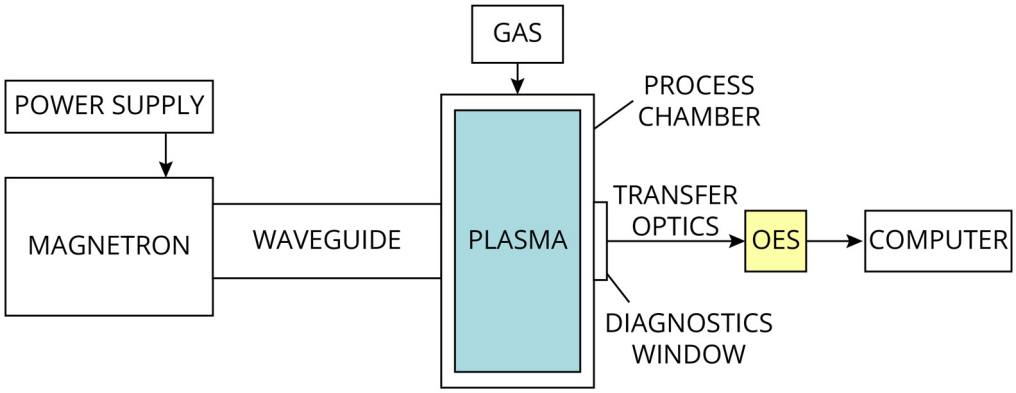

Figure 4. Schematic of microwave-induced plasma–optical emission spectroscopy (MIP-OES).

3.1. Food Quality and Safety Control

An essential aspect of the nutritional and toxicological assessment of food is obtaining information about the concentrations of elements in food. Instant soups are a type of processed food that are easy to prepare and consume, and they also suit a fast-paced lifestyle. The

study [59] used the microwave-induced plasma optical emission spectroscopy (MIP-OES) method to determine Cu, K, Mg, Mn, P and Zn in instant soups. N2 plasma was used, and the samples underwent microwave digestion with a dilute nitric acid solution during preparation. Limits of detection (LODs) were established as follows: Cu (0.09 mg/kg), K (4.90 mg/kg), Mg (1.00 mg/kg), Mn (0.04 mg/kg), P (5.40 mg/kg) and Zn (0.88 mg/kg). The wavelengths of the emission spectrum lines used were: 324.754 nm for Cu, 769.897 nm for K, 285.213 nm for Mg, 403.076 nm for Mn, 213.618 nm for P and 213.857 nm for Zn. Concentrations were determined with good precision (relative standard deviations below 8.4% for all analytes) for all samples: 1.31–13.8 mg/kg for Cu, 1135–17824 mg/kg for K, 172–567 mg/kg for Mg, 1.72–12.1 mg/kg for Mn, 608–1826 mg/kg for P and 2.90–12.1 mg/kg for Zn. MIP OES was recommended for routine analysis of elements in food samples.

Edible mushrooms are a true superfood, as they are rich in proteins, fibres, vitamins and antioxidants, and also contain bioactive compounds such as β-glucan and triterpenes, which strengthen immunity, support heart health and possess medicinal properties. The aim of the study [60] was to develop a method for determining macro- and micronutrients in 11 species of edible and medicinal mushrooms (wild or cultivated from wild strains from the Brazilian Atlantic Forest and commercially medicinal). After wet digestion of edible mushrooms using a closed digestion block, MIP-OES was employed. The results obtained for LODs and LOQs showed good sensitivity of the proposed method for detecting and quantifying the elements of interest: Ca, Cr, Cu, Fe, K, Mg, Mn, Ni and Zn. For each element, the most intense spectral lines were selected: Ca (616.217 nm), Cr (425.433 nm), Cu (324.754 nm), Fe (371.993 nm), K (769.897 nm), Mg (285.213 nm), Mn (403.076 nm), Ni (352.450 nm) and Zn (213.857 nm). The average concentrations in mg/kg of individual elements showed higher levels for K (1442.85–17,534.97), Mg (1295.40–13,550.72), Fe (11.33–27.38), Zn (28.86–36.09) and Mn (10.22–10.97). The results for limits of detection and quantification (LODs and LOQs) showed good sensitivity, precision and accuracy of the proposed MIP-OES method for detecting and quantifying the elements of interest: Ca, Cr, Cu, Fe, K, Mg, Mn, Ni and Zn.

It is known that fish and crustaceans can absorb inorganic elements from soil, sediments, and water. Some of these elements, such as arsenic (As) and mercury (Hg), pose a risk to human health when fish products are consumed. Therefore, it is important to use reliable analytical methods for their determination. In study [61], the use of the MIP-OES method was proposed, with the cold vapour method coupled with the microwave-induced plasma optical emission spectrometry (CV-MIP OES) method for Hg determination, and the hydride generation (HG-MIP OES) method for As determination. Pink shrimp (Penaeus paulensis) and white croaker (Micropogonias furnieri) were sampled from Uruguay. The wavelengths in the emission spectrum were determined: 193.695 nm for As and 253.652 nm for Hg. The limits of detection (LODs) and quantification (LOQs) were estimated for each element. The obtained LOD values were suitable for the planned analysis: 0.0081 mg/kg for Hg and 0.086 mg/kg for As. The results showed that the maximum limits set in the recommendations and legislation were not exceeded: pink shrimp (As 0.21–0.60 mg/kg, Hg not detected); white croaker (As 0.089–0.59 mg/kg, Hg 0.027–0.18 mg/kg).

Chocolate is a food product consumed worldwide in various forms. In the research [62], the authors determined macro- and microelements in 15 chocolate bar samples (Brazilian and imported dark, milk and white chocolate, regular and diet, with different percentages of cocoa) using MIP-OES after microwave digestion of the samples. Limits of detection, quantification, and correlation coefficients of calibration curves are listed for each analyte. The selected spectral lines for each element were at the following wavelengths: 455.403 nm for Ba, 616.217 nm for Ca, 425.433 nm for Cr, 324.754 nm for Cu, 371.993 nm for Fe, 404.414 nm for K, 383.754 nm for Mg, 403.076 nm for Mn, 589.592 nm for Na, 352.454 nm for Ni, 353.560 nm for P, and 213.857 nm for Zn. The determined concentrations were given

in mg/kg: Ca (653–3096); Cr (<0.6–2.8); Cu (<0.16–19.5); Fe (<1.6–227); Mg (147–2775); K (3554–8573); Mn (<0.03–25.2); Na (45.6–1095); Ni (3.2–10.2); P (1111–22,594); and Zn (4.8–33.3). In some samples, the concentrations of Ni and Cr exceeded the values recommended by Brazilian regulations. MIP-OES proved to be a practical and rapid alternative to traditional methods for routine analysis of food samples.

MIP-OES is used for multi-element routine food analysis. Although not as sensitive as some other methods, it is often chosen due to its good performance-to-cost ratio and minimal environmental impact (Table 5).

Table 5. MIP-OES technique: food quality and safety control.

Sample	Determination	Reference
Instant soups	Cu, Mg, Mn, Zn, P	[59]
Wild and cultivated edible mushrooms	Ca, Cr, Cu, Fe, K, Mg, Mn, Ni, Zn	[60]
Pink shrimp (*Penaeus paulensis*) and white croaker (*Micropogonias furnieri*)	As, Hg	[61]
Chocolate bars	Ba, Ca, Cr, Cu, Fe, Ni, Zn, Mn, Mg, Na, P	[62]

3.2. Limitations of MIP-OES: Solutions and Future Developments

Microwave-induced plasma typically operates at lower temperatures (up to 4000–6000 K) compared to ICP (up to 8000–10,000 K), resulting in a lower degree of ionisation due to reduced excitation energy. Consequently, MIP-OES exhibits higher limits of detection than ICP-OES, up to two orders of magnitude worse, making MIP-OES unsuitable for the analysis of trace elements and those requiring higher ionisation energy (such as non-metals). Limits of detection depend on the sample matrix and preparation method, but typical values vary from µg/L to mg/L [62,63]. Commonly used analytical lines in MIP-OES for some elements with a reported value of LOD from [58] are shown in Table 6. For most elements, the limits of detection for MIP-OES are comparable to those for ICP-OES.

Table 6. Representative emission lines for some elements in MIP-OES technique.

Element	Wavelength (nm)	LOD (µg/L or ppb)
Aluminium (Al)	396.152	0.7
Calcium (Ca)	422.673/317.933	13
Copper (Cu)	324.754/327.396	0.3
Iron (Fe)	248.327/371.993	4
Potassium (K)	766.491/769.897	118
Magnesium (Mg)	285.213/518.360	1.1
Manganese (Mn)	279.482/280.106	0.4
Sodium (Na)	588.995/589.592	600
Phosphorus (P)	213.618/214.914	7550
Zinc (Zn)	213.857	3

In complex sample matrices, spectral interferences (emission of molecular bands, e.g., NO bands affecting Zn determination) can suppress or enhance the measured emission intensity, complicating quantitative analysis, particularly with a lower spectral resolution. Complex spectra necessitate the careful selection of wavelengths corresponding to the emission lines of the elements being analysed [64,65].

When using argon in MIP-OES for the detection of metals such as Ca, Mg, Fe and Cu at an LOD of 10 µg/L, there are discrete peaks at the expected wavelengths in the emission spectrum with a high signal-to-noise ratio. The interference of spectral lines of different elements is minimal due to the spectral resolution and plasma environment with excited Ar atoms that is easy to analyse. The use of nitrogen as a working gas in the detection of

non-metals such as P and S enhances the emission, and the spectra show pronounced lines of high intensity at 178.2 nm for P and at 180.7 nm for S.

Improved sample introduction into the plasma is necessary to ensure signal stability, for example, by using low-flow nebulisers or aerosol dilution techniques. Optimised cavity design can enhance plasma stability and analytical performance. High-resolution detectors combined with background correction algorithms can reduce spectral interferences and improve quantification accuracy. MIP-OES can be used alongside ICP-OES, with the former serving for screening and routine analyses in industrial quality control, and the latter for the confirmation and quantification of trace elements.

Future research should focus on higher-power microwave sources to improve excitation and expand analytical capabilities. The most commonly used gases are nitrogen, argon and air, and experimental studies with mixed gas plasmas (such as nitrogen/helium or nitrogen/hydrogen) are proposed to increase excitation efficiency and reduce spectral interferences. The use of artificial intelligence methods enables the automation of spectral line selection based on previously learned models and assists in removing interferences. The miniaturisation of MIP-OES systems that are mobile and suitable for various laboratory and industrial environments, including on-site applications, is also envisaged.

4. Dielectric Barrier Discharge–Optical Emission Spectroscopy (DBD-OES)

Dielectric barrier discharge (DBD) is a straightforward method for generating plasma at atmospheric pressure. The discharge is blocked by a dielectric barrier layer (such as glass, quartz, ceramics, polymers, or plastics) and can be implemented in several ways: covering one electrode, both electrodes (Figure 5), or positioned in the space between the electrodes. Charge transfer and conductive current are limited. Most often, an AC voltage across a wide frequency range (up to 1 MHz) is used to initiate the discharge. DBD geometry can vary (coaxial, surface, planar, etc.), but the operating principle remains the same: electrons accelerated by the applied electric field collide with neutral molecules, initiating the ionisation process and creating plasma. The sample is placed between the electrodes and is thus directly exposed to the generated plasma. Numerous parameters affect processing efficiency, including pressure, gas type, flow rate, DBD geometry, and sample characteristics. However, the advantages of DBD include low energy consumption; a simple, compact design; and a wide range of applications [66,67].

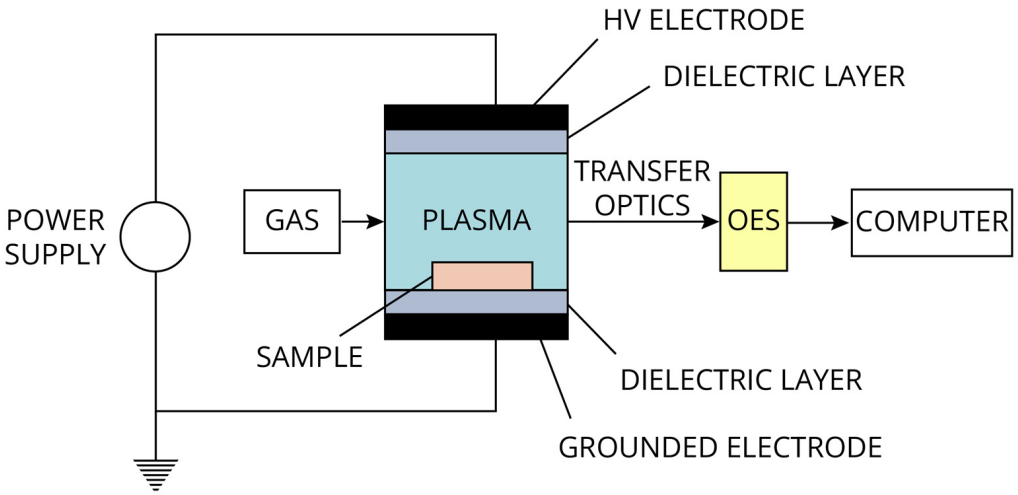

Figure 5. Schematic of dielectric barrier discharge–optical emission spectroscopy (DBD-OES).

4.1. Decontamination in the Food Industry

Since the DBD system generates plasma at an atmospheric pressure using gases such as air, nitrogen, oxygen, argon, or mixtures of these gases, there is no need to provide vacuum conditions. The resulting plasma is a cold or non-thermal plasma, rich in reactive oxygen and nitrogen species (RONS) such as atomic oxygen, ozone, hydroxyl radicals, nitric oxide, and nitrogen dioxide, and is safe for use on heat-sensitive materials [68]. The synergistic action of RONS with UV radiation, charged particles, and local electric fields that occur in plasma systems is used to inactivate a wide range of microorganisms (spores, fungi, bacteria, viruses) in the food industry without chemical disinfectants [11,69]. The role of OES is to monitor and characterise the plasma system during DBD decontamination. OES identifies characteristic emission lines and molecular bands (such as OH(A-X), N_2 (second positive system), N_2^+ (first negative system)), as well as plasma composition and relative species density. The information provided by OES as a non-invasive, real-time sensor enables a correlation between operational parameters for DBD plasma technology (working gas, applied voltage, frequency, treatment time) and decontamination efficiency [12].

Mycotoxins, as natural contaminants of cereals, are a group of secondary metabolites produced by moulds that, due to their toxic, neurotoxic, and carcinogenic properties, pose a threat to human and animal health and present a challenge for food safety and quality. The T-2 toxin and its main metabolite, the HT-2 toxin, belong to a large group of trichothecene mycotoxins synthesised by various Fusarium species. The authors of a prior study [70] focused on the effectiveness of low-pressure DBD plasma in degrading T-2 and HT-2 toxins in oat flour. Measurements were carried out using different working gases (argon, air, oxygen, and nitrogen) and various exposure intervals (10, 20, and 30 min). The formation of reactive gas species with oxygen as the working gas was monitored by OES. Initially, the spectrum of pure oxygen plasma showed spectral lines of oxygen atoms at 615.6 nm, 777.2 nm, and 844.6 nm, as well as molecular bands of transitions of molecular oxygen ions O_2^+ with band heads at 526 nm (2,0), 560 nm (1,0), 598 nm (0,0), and 639 nm (0,1). After placing the sample in the reactor, the spectrum changed significantly and initially showed only hydrogen lines at 656.2 nm (H_α) and 483 nm (H_β). Further treatment with DBD plasma also altered the spectral image, with increased intensity of oxygen lines, weakened hydrogen lines, and the appearance of CO molecular bands (Angstrom band: 451.1 nm (0,0), 483.5 nm (0,1), 519.8 nm (0,2), 561 nm (0,3), 608 nm (0,4), and 662.1 nm (0,5)), and in the UV spectrum, overlapping N_2 molecular bands at 315.9 nm (1,0), 337.1 nm (0,0), and 357.7 nm (0,1) (second positive band), as well as the third positive CO band at 312.9 nm (0,2), 330 nm (0,3), and 348.8 nm (0,4). The importance of monitoring oxygen plasma using OES was demonstrated, as it provided insight into the influence of sample humidity on the efficiency of oxygen atomisation during treatment.

A similar study [71] was conducted on the degradation of zearalenone by cold plasma dielectric barrier discharge. Zearalenone is an oestrogenic mycotoxin produced by Fusarium and is one of the most widespread mycotoxins contaminating maize, wheat, other cereals, and their products. In this research, OES was also used to obtain qualitative information about reactive species in the plasma. Air was used as the working gas, and the emission spectrum was dominated by the second positive system N_2 (N_2 (C–B)) at 300–430 nm. Oxygen was not detected, but a weak OH peak was recorded near 295–300 nm, generated from moisture in the air. During the formation of cold plasma, reactive species of different wavelengths can cause dissociation of the covalent bonds in zearalenone, thereby destroying its original molecular structure. Additionally, OES measurements were performed at different operating voltages for plasma production (35 kV, 40 kV, 45 kV, 50 kV). The same reactive species were observed at different voltages, but increasing the voltage also increased the intensity of the spectral lines. This increased the number of active species

and the rate of zearalenone degradation. Without OES, such information could not be obtained and the parameters of DBD plasma decontamination could not be optimised.

DBD plasma technology is also used as a non-thermal method for the decontamination and preservation of fresh food products (fruits and vegetables) by generating reactive oxygen and nitrogen species (RONS) that inactivate microorganisms without chemicals or additional heating. Research [72] showed that the application of cold DBD plasma technologies in packaging is relatively effective in reducing the original microflora on fresh-cut carrots. OES enabled the identification and study of excited species in plasma, as plasma spectroscopy was performed when the samples were treated at three different voltages. Intense peaks were observed in the wavelength range 315–405 nm, identified as transitions from the second positive nitrogen system, N_2 (C–B) (at 336.9 nm, 357.3 nm, 380.0 nm, and 405.4 nm), and the first negative system, N_2^+ (B–X) (at 390.6 nm and 427 nm, with relatively low intensities). Plasma emission in the UV region was very limited, so the action of reactive gas species dominated in this region, as confirmed by OES.

The integrated DBD-OES system has wide and effective applications in the food industry because it enables the optimisation and reproducibility of decontamination treatments (Table 7). Process control and monitoring by OES ensure that plasma stability is maintained with the appropriate number of reactive species generated. DBD-OES is proving to be an excellent alternative to conventional decontamination technologies closely related to food safety [69].

Table 7. DBD-OES: decontamination in food industry.

Sample	Determination	Reference
Oat flour	O, O_2^+, H_α and H_β, CO, N_2^+	[70]
Zearalenone	N_2 (C–B), N_2 (C–X), O, OH, NO	[71]
Fresh-cut carrots	O, OH, N_2, N_2^+	[72]

4.2. Limitations of DBD-OES: Solutions and Future Developments

DBD-OES has several applications in the food industry: the detection of heavy metals in liquid samples and water, trace metal analysis with nebulisation, determination of halogens in certified reference materials, detection of additives in processed foods, etc. Depending on the food sample being analysed, the method of introducing the sample into the DBD-OES system, and the element to be tested, representative emission lines and associated detection limits are used (Table 8) [73–76].

Table 8. Representative emission lines for some elements in DBD-OES technique.

Element	Wavelength (nm)	LOD (μg/L or ppb)
Bromine (Br)	827	11
Cadmium (Cd)	228.8	1.6
Chlorine (Cl)	837	15
Iodine (I)	905	95
Mercury (Hg)	253.7	10
Sulphur (S)	301.9	10
Zinc (Zn)	213.9	22

In classic systems, the focus is on the quantification of elements, but DBD systems produce cold or non-thermal plasma that is suitable for decontamination in the food industry [77–80]. Then OES becomes a diagnostic tool for identifying reactive nitrogen and oxygen species that are responsible for enzyme inactivation in food, lipid oxidation and destruction of the cell membrane of microorganisms. An overview of species and wavelengths is given in Table 9 [81,82].

Table 9. Representative emission lines for some species in DBD-OES technique.

Species	Wavelength (nm)
Second positive system of N_2 ($C^3\Pi_u \rightarrow B^3\Pi g$)	300–500
First positive system of N_2 ($B^3\Pi g \rightarrow A^3\Sigma_u^+$)	630–900
First negative system of N_2^+ ($B^2\Sigma_u^+ \rightarrow X^2\Sigma g^+$)	~393
Nitrogen N I	~818.6
Oxygen O I	~777, ~844
Hydroxyl OH	306–310
Nitric oxide NO	200–300
Helium He I	388.9, 492.2, 587.6
Hydrogen H_α	656.3

In DBD systems, the intensity of OH radicals correlates with the efficiency of decontamination. In this case, OES is used to monitor and control the parameters that affect OH generation (applied voltage and frequency, pressure, humidity). Increasing the applied voltage will directly increase the intensity of the OH line by providing enough kinetic energy to dissociate water vapour molecules in collisions. Pressure affects the mean free path of electrons, i.e., the distance an electron travels between two collisions. The intensity of the OH line increases with increasing humidity until a critical point when excessive humidity, by trapping free electrons, begins to reduce their energy and thus the intensity of the OH line in the optical emission spectrum. A higher frequency results in higher plasma density and higher OH emission intensity while maintaining the stability of the plasma system without heating the food sample. The physics of the discharge changes with the choice of the working gas, which is associated with the method of controlling the parameters that are important for plasma generation. Air is shown to be more economically viable, but noble gases such as argon or helium provide a significantly more stable plasma, which is an important factor in the application of plasma technology. Argon ionisation occurs at lower voltages, and the produced plasma covers the entire surface of the food, which allows for very precise control of radical formation. Air ionisation requires a higher voltage because oxygen and nitrogen are diatomic molecules, and the result may be non-uniform decontamination or even partial damage to the food surface. The solution to these problems may be an appropriate gas mixture that will provide a stable plasma and an increased yield of reactive species [69,83].

The main limitation of the DBD-OES system arises from the spatially and temporally inhomogeneous DBD plasma, which causes fluctuations in emission intensity. Consequently, quantitative analysis of species concentrations is unreliable because the obtained spectra are not representative or reproducible. The measured spectra are complex due to the wide range of excited species generated in the plasma (ions, atoms, radicals, molecular bands), resulting in overlapping spectral lines and making it impossible to identify lines of lower intensity. The dynamics and properties of the plasma can also be influenced by surface effects and interaction with the dielectric material.

The use of time- and spatially resolved OES can reduce the impact of plasma inhomogeneities by isolating specific discharge regions. The problem of spectral line overlap can be addressed by using high-resolution spectrometers and spectral deconvolution methods. Employing collisional–radiative models with OES measurements improves the interpretation of the spectra and enables more reliable quantitative analysis. Plasma characterisation can also be enhanced by the parallel use of DBD-OES and complementary diagnostics such as mass spectrometry or electrical measurements. Despite these intrinsic limitations, the further development and continued use of DBD-OES systems, combined with machine

learning that uses large datasets to build models capable of independently predicting results for new, unknown data, is expected in the future.

5. Plasma Jet–Optical Emission Spectroscopy (PJ-OES)

The plasma jet (PJ) operates on a principle similar to that of dielectric barrier discharge (DBD), with the distinction that the reactor is cylindrical and made of dielectric material. Two electrodes are arranged in a ring, with one necessarily grounded. The working gas, usually an inert gas or a gas mixture, enters at one end of the reactor and flows at a high rate through the centre of the cylinder, where it is ionised (Figure 6). The resulting plasma jet, rich in reactive species, exits at the other end of the reactor into open space, where the sample to be treated is placed. By adjusting the operating parameters—voltage amplitude, power supply frequency, and gas flow rate—a stable plasma jet is maintained. The advantages of PJ include operation in an unrestricted area, the ability to treat various materials, and the fact that the sample no longer needs to be inside a closed system containing the plasma source. Separating the plasma source from the interaction area between the plasma and the sample enables the monitoring and control of the plasma dynamics, which is achieved using optical emission spectroscopy (OES). PJ is most commonly used in biomedicine, for sterilisation, and for material processing [57,84].

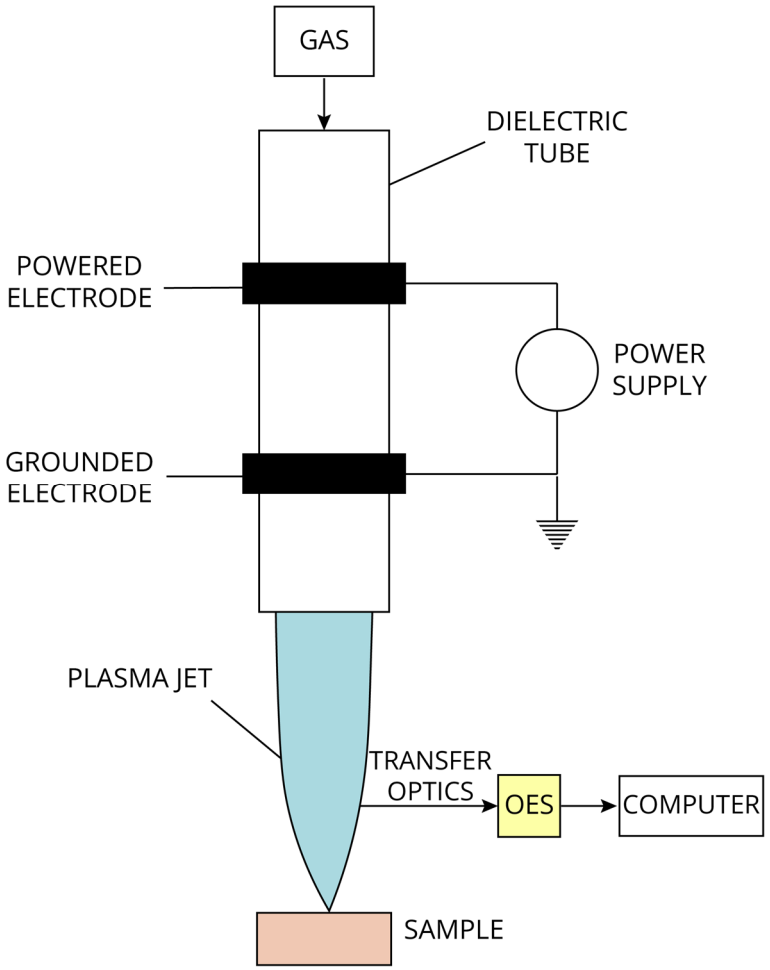

Figure 6. Schematic of plasma jet–optical emission spectroscopy (PJ-OES).

5.1. Decontamination and Food Safety Control

A study [85] evaluated the effect of atmospheric pressure plasma jet treatment on the morphology of wheat seeds (*Triticum aestivum* L. 'Dacic' and 'Otilia'), their germination,

biochemical composition, and the nutritional quality of wheatgrass. UV-NIR plasma spectroscopy (200–900 nm) showed that the plasma source used had sufficient energy to excite not only the lines of the working gas (helium in this case) but also the lines and bands of other atmospheric species such as NO_γ, OH, N_2, N_2^+, and O. These reactive nitrogen and oxygen species (RONS) play a significant role in the interaction of plasma with the sample surface. In the 200–300 nm interval, the NO_γ lines dominated at 237 nm, 247 nm, 259 nm, and 271 nm. At 309 nm, a rotational band of hydroxyl radicals (OH) was observed. In the 315–390 nm interval, molecular nitrogen (N_2) bands were found at 315 nm, 337 nm, 357 nm, and 375 nm. At 391 nm, a molecular nitrogen ion band (NO_γ, OH, N_2, N_2^+) was detected, which was important for estimating the gas temperature using the Boltzmann plot. Molecular ion bands were again found in the 400–470 nm region, but with weaker intensity. Helium spectral lines were detected in the 580–740 nm interval: 588 nm, 668 nm, 706 nm, and 727 nm. Atomic oxygen lines were also identified at 777 nm and 845 nm. The importance of the precise spectroscopic detection of excited species along the spectral lines of the working gas was demonstrated to determine whether, and under what conditions, they will be used for sample treatment.

During processing, packaging, and storage, food comes into contact with various materials that may harbour pathogenic microorganisms. The migration of microorganisms into food leads to contamination, affecting the safety and quality of food. Therefore, it is important to inactivate these microorganisms both quickly and effectively. Cold atmospheric plasma (CAP) has been shown to be an effective non-thermal sterilisation technology. A study [86] investigated the inactivation effect of atmospheric helium plasma jet treatment on *Salmonella typhimurium* and *Staphylococcus aureus* populations on three food contact materials (kraft paper, 304 stainless steel, and glass). The emission spectrum of the plasma jet showed that CAP generates many active species, including radicals, ions, excited molecules, and UV photons. In addition to the prominent He (He I) lines in the excited state (at 501.50 nm, 587.50 nm, 667.80 nm, 706.50 nm, and 728.13 nm), other emission lines were observed, including OH ($A^2\Sigma \rightarrow X^2\Pi$) at 309 nm; N2 s positive band ($C^3\Pi_u \rightarrow B^3\Pi_g$) at 315.93 nm, 337.13 nm, 357.69 nm, and 380.49 nm; N_2^+ first negative ($B^2\Sigma_u \rightarrow X^2\Sigma_g$) at 391.44 nm, 427.81 nm, and 470.92 nm; the Balmer line H_α at 656.30 nm; and O (3p5S–3s5S) lines at 777.53 nm and 844.63 nm. Due to their properties, RONS play an important role in the microbial inactivation process, as demonstrated by plasma spectroscopy.

Phytopathogens frequently cause crop yield losses, prompting scientists to develop new pest eradication methods that are also environmentally friendly. Cold atmospheric plasma, applied as a plasma jet with optimised working conditions, has proven to be an effective inactivation method in research [87]. The bacterial phytopathogens *Dickeya solani*, *Pectobacterium atrosepticum* and *Pectobacterium carotovorum* were treated on the surfaces of plant seeds from the following species: *Cucumis sativus*, *Pisum sativum*, *Vigna radiata* and *Zea mays*. Optical plasma emission spectroscopy was used to identify reactive oxygen species (ROS) and reactive nitrogen species (RNS) produced during atmospheric pressure plasma jet (APPJ) application. In the 200–400 nm (UV) region, the emission bands of OH (A–X) (at 282.9 nm (1–0 transition) and at 308.9 nm (0–0 transition)); N_2 (C–B) (at 315.9 nm (1–0), 337.1 nm (0–0), 353.7 nm (1–2), 357.7 nm (1–2), 375.5 nm (1–3) and 380.5 nm (0–2)); and a strong N_2^+ (B–X) band at 391.4 nm (0–0) were excited. In the 400–900 nm range, the atomic lines of He as a working gas (He I) were detected at 587.5 nm, 667.8 nm, 706.5 nm and 728.1 nm; the H lines at 486.1 nm and 656.2 nm; and the atomic lines of O (O I) at 777.2 nm, 772.4 and 844.6 nm. By the combined application of colorimetric tests and optical emission spectrometry (OES), the oxidative potential was determined with the identification of reactive oxygen species (ROS) •OH, $\bullet HO_2$, $\bullet O_2^-$, O_3 and $^1O_2$ and reactive nitrogen species (RNS) N, NO_2 and NO_3, which are responsible for the antibacterial properties of APPJ.

In research on water treatment using the atmospheric pressure cold plasma method, it is generally accepted that, in most applications, the effects induced by plasma came from the action of reactive oxygen and nitrogen species (RONS). In study [88], water with and without buffer was treated using a plasma jet, with argon as the working gas and three adjustable parameters: applied voltage amplitude, applied voltage frequency, and gas flow rate. OES was used to investigate the generated species whose emission is detected in the UV-NIR region: excited molecular nitrogen N_2 (SPS): $C^3\Pi_u \rightarrow B^3\Pi_g$ (at 337.13 nm, 357.69 nm, 380.49 nm); hydroxyl OH: $A^2\Sigma^+ \rightarrow X^2\Pi$ at 309 nm; and excited argon atoms (16 Ar I lines from 696.54 nm to 922.45 nm). The rotational distribution of the hydroxyl molecule, OH (A), was experimentally recorded and numerically reproduced, which is accepted as a reliable molecule for rotational temperature measurements. The average gas temperature along the plasma jet was estimated to be about 350 ± 40 K. In the paper, the optical emission intensities of the main emissive species (N_2, OH, Ar) were measured as functions of the applied voltage amplitude, applied voltage frequency and argon flow rate.

PJ-OES is an excellent method for decontamination and food safety control because it provides real-time diagnostics, thus enabling the advancement of plasma technology applications (Table 10).

Table 10. PJ-OES technique: decontamination and food safety control.

Sample	Determination	Reference
Wheat seeds (*Triticum aestivum* L.)	NO_γ, O, OH, N_2, N_2^+	[85]
Food contact materials (kraft paper, 304 stainless steels, glass) with *Salmonella typhimurium* and *Staphylococcus aureus* populations	He I, O, OH, N_2^+	[86]
Plant seeds of the species *Cucumis sativus*, *Pisum sativum*, *Vigna radiata* and *Zea mays*	OH, N_2, N_2^+, H, He, O	[87]
Buffered or unbuffered water	OH, N_2, Ar I	[88]

5.2. Limitations of PJ-OES: Solutions and Future Developments

Atmospheric pressure plasma jets (APPJ) are non-thermal plasmas used in the food industry for surface decontamination, microbiological inactivation, and the preservation of nutritional and sensory quality. OES-PJ provides information on the production of reactive oxygen and nitrogen species necessary for the decontamination of heat-sensitive food samples. The most commonly used atmospheric pressure plasma jet based on argon or helium in the optical emission spectrum will give peaks of hydroxyl radicals, atomic oxygen, molecular nitrogen, nitric oxide and nitrogen ion at the same wavelengths as given in Table 9 for the DBD-OES technique. When using argon, strong emission lines are detected in the NIR region (700–850 nm), especially at 696.5 nm, 706.5 nm, 750.4 nm and 811.5 nm. The standard in treating food with a plasma jet is the use of air or a mixture of argon and air. A high O/N_2 ratio in surface decontamination with APPJ gives a higher efficiency due to strong oxidation of the cell membrane. High intensities of N_2^+ and NO systems can affect the nutritional value of food, so the treatment time can be optimised by using OES. If the system is dominated by argon lines, most of the electron energy goes to the excitation of the inert gas, and not to the creation of chemically active species. OES monitoring enables flow optimisation to enable the desired effect of plasma jet action [89–93].

Although widely used, plasma jet–optical emission spectroscopy (PJ-OES) systems face several limitations. The localised processing of food surfaces or packaging materials with laboratory spectral diagnostics is performed on small-volume samples under strictly controlled conditions. Scaling PJ-OES diagnostics to industrial volumes is constrained by

the size of the instrumentation and the requirements for monitoring sensitivity. In addition to the wide range of excited species in the plasma jet, including reactive oxygen and nitrogen species, interpretation of the emission spectrum is complicated by the atmospheric pressure environment and line broadening. The presence of overlapping lines in complex spectra makes species identification and quantitative analysis challenging. Environmental factors such as humidity or background nitrogen and oxygen can alter the intensity of emission lines, making it difficult to identify those resulting from the plasma–food interaction.

Although PJ-OES is used as a qualitative technique, with rigorous calibration to reference standards and well-defined protocols, its quantitative capabilities can be improved, for example, by translating emission line intensities into concentrations of reactive species and thus monitoring plasma jet efficiency. The use of high-resolution, time-resolved spectrometers is also proposed, as these reduce line overlap and allow for the isolation of emission lines during different phases of plasma evolution. In future, it is envisaged that large databases obtained from spectral measurements will be used for predictive modelling with machine learning, facilitating adaptive process optimisation in industrial environments.

6. Determination of the Applied Plasma Parameters Using OES

6.1. Determination of the Temperature of the Applied Plasma Using OES

The plasma system is in thermodynamic equilibrium if all types of particles have the same temperature and there are no temperature or density gradients. Due to thermal equilibrium, the number of atoms in any quantum state is given by the Boltzmann distribution [26]:

$$N_n \sim \exp(-\frac{E_n}{k_B T}) \tag{1}$$

or by the Boltzmann factor:

$$\frac{N_m}{N_n} \sim \exp\left(-\frac{E_m - E_n}{k_B T}\right) = \exp(-\frac{h\nu}{k_B T}) \tag{2}$$

where N_n and N_m are populations of energy states n and m, E_n and E_m associated energies, $k_B T$ thermal energy, k_B Boltzmann constant, T temperature, $h\nu$ energy of the emitted photon during the transition from a higher to a lower level $m \rightarrow n$, h Planck's constant, and ν frequency of the emitted photon. Levels n and m consist of a certain number of degenerate states, so the statistical weights of levels g_n and g_m are introduced:

$$N_n \sim g_n \exp(-\frac{E_n}{k_B T}) \tag{3}$$

$$\frac{N_m}{N_n} \sim \frac{g_m}{g_n} \exp\left(-\frac{E_m - E_n}{k_B T}\right) = \exp(-\frac{h\nu}{k_B T}) \tag{4}$$

In thermal equilibrium, the radiation spectrum is described by Planck's law. In a stationary field, the total number of transitions from level n to level m must be equal to the total number of transitions from m to n. This represents the principle of detailed equilibrium which satisfies Planck's law at all temperatures. Real plasmas, produced for laboratory research or for industrial applications, are in local thermodynamic equilibrium (LTE) where different particles may be at different temperatures, but locally, within a smaller area, the plasma system can be considered to be in equilibrium. Sometimes this condition is too strict, so partial local thermodynamic equilibrium (PLTE) is assumed, in which different subsystems (such as electrons, ions, and atoms) can be in different local equilibria, meaning they are at different temperatures (e.g., T_e, T_i, T_a). Bound electrons populate discrete energy levels in accordance with the Boltzmann distribution, and the density of free particles

follows the Saha relation [94], which describes the degree of ionisation in a plasma in thermal equilibrium, connecting populations of different ionisation states (e.g., neutral atoms versus ions) with temperature, electron density, and ionisation energy. If we consider two spectral lines 1 and 2 coming from the same atomic or ion sample (Figure 7), and if the level populations are given by Boltzmann's law, the electron temperature can be determined from the ratio of the relative intensities of the spectral lines:

$$\frac{I(1)}{I(2)} = \frac{A_{mn}(1)}{A_{mn}(2)} \frac{g_m(1)}{g_m(2)} \frac{\lambda_0(2)}{\lambda_0(1)} \exp\left(-\frac{E_m(1) - E_m(2)}{k_B T}\right) \quad (5)$$

where $I(1)$ and $I(2)$ are the relative line intensities, $A_{mn}(1)$ and $A_{mn}(2)$ are the transition probabilities, m is the higher line level, n is the lower line level, $g_m(1)$ and $g_m(2)$ are the statistical weights of the higher levels, $\lambda_0(1)$ and $\lambda_0(2)$ are the wavelengths of the line centres, and $E_m(1)$ and $E_m(2)$ are the energies of the higher line levels.

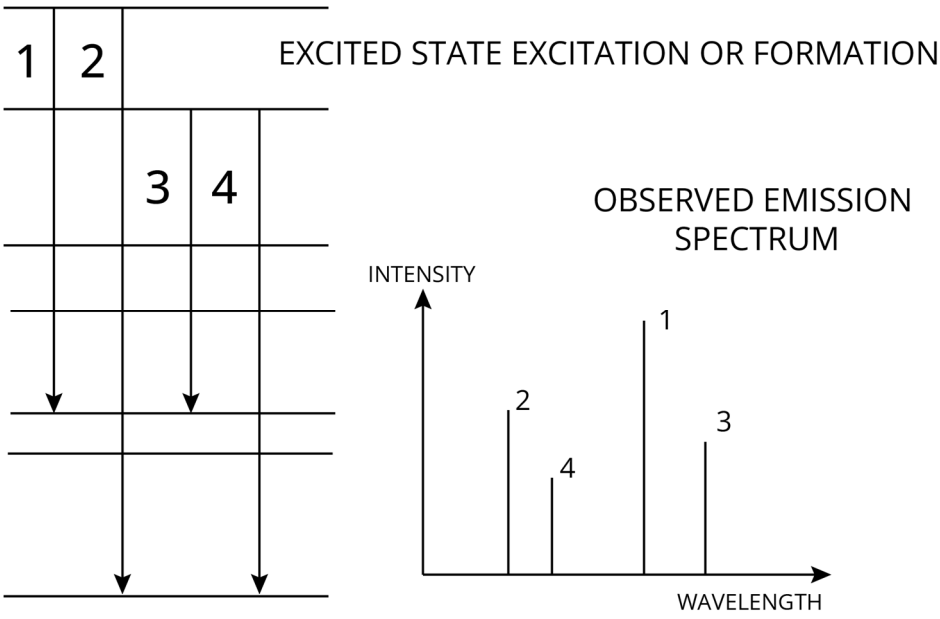

Figure 7. Energy levels in emission spectrum.

The main problem with this method is the small energy difference between the higher levels of spectral lines of the same ionisation state. The electron temperature can also be determined from the ratio of the relative intensities of spectral lines of the same element, but from successive ionisation states, as the relevant energy difference is increased by the ionisation energy, which is usually higher than $k_B T$. In this case, the electron density must be known to determine the electron temperature. One approach is to initially assume values for the electron temperature and electron density that have been obtained by measurement or estimation.

Determining the electron temperature from the relative intensities of the spectral lines of the same atomic sample is a very simple method, as it requires measuring only the relative line intensities, which is easier than measuring their absolute values. The calculated temperatures do not depend on the plasma parameters; however, the accuracy of the results is limited because the ratio of line intensities becomes insensitive to temperature in the high-temperature region. Accuracy can be improved by using the Boltzmann plot method, where the level populations are plotted on one axis and the higher-level energies on the other:

$$\ln\left(\frac{I_{mn}\lambda_{mn}}{g_m A_{mn}}\right) = -\frac{1}{k_B T} E_m + \ln\left(\frac{4\pi Z}{hcN_m}\right) \quad (6)$$

where Z is the partition function, and c is the speed of light. Spectral lines of higher intensity are selected. The result is the slope coefficient $\left(-\frac{1}{k_B T}\right)$ and the accuracy is improved by fitting the slope using the standard linear regression method [26,95]. Experimental OES measurements provide data for λ_{mn} and I_{mn}, and the values of g_m, A_{mn} and E_m for the corresponding λ_{mn} can be obtained from the National Institute of Standards and Technology (NIST) [96].

6.2. Determination of the Density of the Applied Plasma Using OES

Spectral lines emitted by ions or atoms in plasma can be broadened in several ways. One such mechanism is Stark broadening, which occurs due to the varying local electric fields of nearby charged particles (ions and electrons) [97]. These electric fields interact with the emitting ion or atom, causing the splitting or shifting of its energy levels. As the fields change rapidly, the wavelength (or frequency) of the emitted radiation is not a single sharp line but a broadened distribution, the width of which is related to the field strength and the density of the charged particles. Two broadening regimes are usually considered: the first is associated with quasi-static electric fields caused by ions, and the second with fast collisions between electrons and other radiating species. For most laboratory plasmas with electron densities above 10^{14} cm^{-3}, such as those used in the food industry, the second regime is dominant. When the Stark broadening mechanism is dominant and other broadening mechanisms (Doppler, strong, natural, instrumental) are small or negligible, the Stark broadening is well approximated by a Lorentzian profile with width determined by electron-impact broadening [98]. The Lorentzian profile (Figure 8) describes homogeneous broadening mechanisms:

$$I(\lambda) = I_0 \frac{\left(\frac{FWHM}{2}\right)^2}{(\lambda - \lambda_0)^2 + \left(\frac{FWHM}{2}\right)^2} \quad (7)$$

where λ_0 is the central wavelength, $FWHM$ is full width at half maximum of intensity, and I_0 is the maximum intensity (peak).

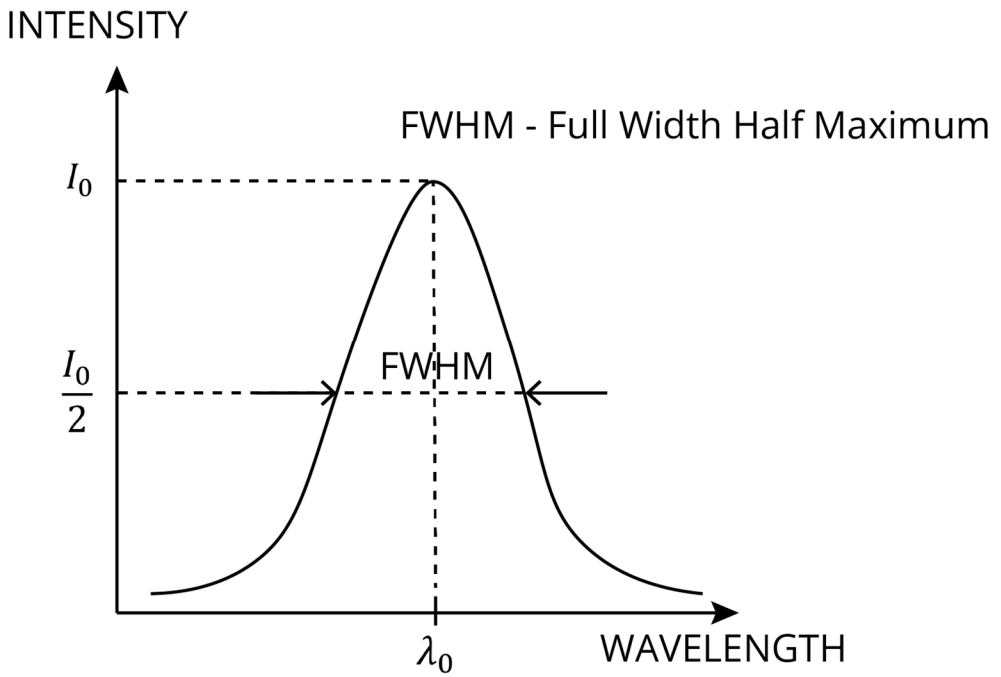

Figure 8. Lorentzian profile.

Also, $FWHM$ can be directly related to electron density n_e:

$$n_e = \frac{FWHM}{2w} \times 10^{16}\ \mathrm{cm}^{-3} \quad (8)$$

where w is the electron impact Stark broadening parameter (in angstroms Å), tabulated for specific transitions and temperatures [99].

The study [100] demonstrates the efficient use of the APPJ system for the simultaneous and uniform treatment of large chilli seeds. A new configuration, designed based on the dielectric barrier discharge (DBD) principle, was developed to enable scalable plasma exposure over an extended surface area. However, to understand the mechanisms of the plasma–seed interaction, identify active species, and determine key plasma parameters, diagnostics using OES were performed. The emission spectrum (250–950 nm) was dominated by emission lines of argon, used as the working gas, and by reactive oxygen species responsible for modifying the seed surface, as well as reactive nitrogen species resulting from the interaction of the plasma jet with the surrounding air. To determine the electron temperature, the ratio of the relative intensities of two spectral lines of the same atomic species (Ar I lines at 706.7 and 810.3 nm) was used, yielding a value of 1.4487 eV. To determine the electron density, the Boltzmann and Saha equations were applied to the intensity ratios, resulting in a value of 3.4867×10^{15} cm^{-3}. OES confirmed the creation of a sufficiently dense and energetic plasma capable of effectively modifying the surface of chilli seeds.

A DBD-based cold argon APPJ was used in study [17] to modify the surface of white grapes. Comprehensive electro-optical characterisation of the plasma and optimisation of discharge parameters were performed using OES in combination with the collision–radiation model. Optical emission spectra showed the generation of various species (Ar I, N I, O I, N_2, OH, etc.) and enabled the calculation of electron temperature (~1 eV) and electron density (~10^{14} cm^{-3}). It was shown that relatively high density is responsible for the effective formation of RONS in the jet surroundings. To determine the rotational temperature T_{rot}, often considered as the gas temperature T_{gas}, the Boltzmann plot for the OH emission band was used, yielding a value of ~310.5 K, which demonstrates the non-equilibrium nature of cold argon APPJ under the optimised conditions of applied voltage, frequency, and argon flow rate. Plasma treatment modified the physical characteristics on the surface of white grapes without causing chemical degradation, highlighting its suitability for the non-thermal and non-destructive processing of fresh products.

Study [101] presents the development and comprehensive characterisation of an atmospheric pressure gliding arc plasma jet (GAPJ), which is successfully used for decontamination in the food industry. The generated non-thermal plasma operated at atmospheric pressure in ambient air. The electron excitation temperature was determined using the Boltzmann plot, with values in the range (1.36–1.44) eV. Rotational and vibrational temperatures under various operating conditions were analysed, with the following intervals obtained: T_{rot} (1373–2065) K and T_{vib} (2405–2700) K. Rotational and vibrational temperatures in plasma provide information on the distribution of the kinetic energies of molecular motion and on the classification of plasma as thermal or non-thermal, indicating suitability for food applications. The electron density range (0.62–3.44) $\times 10^{19}$ m^{-3} was also estimated. OES confirmed that this is a non-thermal plasma suitable for the decontamination and sterilisation of heat-sensitive surfaces.

Study [102] demonstrated the need for the monitoring and diagnostic of non-thermal argon plasma, often applied in food processing. High-voltage electrical discharge (HVED)-generated plasma is mostly used for the extraction of bioactive components or for the inactivation of microorganisms. OES, as a non-invasive sensor, enabled the identification of

excited species from the measured emission spectra. Using the Boltzmann plot method and Ar I and Ar II spectral lines, electron temperature values of (2.1 ± 0.2) eV were obtained, confirming that it is a non-thermal plasma suitable for use in the food sector. Based on the assumptions of partial local thermodynamic equilibrium (PLTE), the electron density was estimated, ranging up to 10^{23} m^{-3}. As OES provides information in near-real time, it can be used to optimise the process parameters of non-thermal plasma technology, ensuring increased efficiency, effectiveness, and sustainability.

Optical emission spectroscopy is a diagnostic tool for determining temperature and density in plasma, which is used for decontamination and analysis of the quality and safety of food products. The data obtained are also used for the optimisation of operational parameters (Table 11).

Table 11. Electron temperature and density determination by OES.

Technique	Gas	Electron Temperature	Electron Density	Reference
DBD-OES	Ar	1.4487 eV	3.4867×10^{15} cm^{-3}	[100]
DBD-OES	Ar	~1 eV	~10^{14} cm^{-3}	[17]
GAPJ-OES	air	(1.36–1.44) eV	(0.62–3.44) × 10^{19} m^{-3}	[101]
HVED-OES	Ar	(2.1 ± 0.2) eV	up to 10^{23} m^{-3}	[102]

6.3. Limitations to the Determination of the Parameters of Plasma Applied in the Food Industry: Solutions and Future Developments

Temperature control of the applied plasma in the food industry is important because it ensure the preservation of food quality, affects the efficiency of decontamination, and aids in process optimisation. As non-thermal or cold plasma is used in food processing, accurate diagnostics confirm the temperature range in which thermal damage to the samples will not occur, while sensory and nutritional properties are preserved. A key limitation of optical emission spectroscopy (OES) for determining plasma temperature arises from the non-equilibrium nature of non-thermal plasma, as electrons can have significantly higher temperatures than ions and neutral particles. Therefore, it is important to consider the assumptions of local thermodynamic equilibrium (LTE) or partial local thermodynamic equilibrium (PLTE) when determining the temperature using the Boltzmann plot method or the ratio of relative intensities of spectral lines. In plasmas with multiple ionised species, differences in the intensities of emission lines are significant, affecting the signal-to-noise ratio and signal quality, and thus, indirectly, the determination of temperature. Different plasma system geometries can result in spatial gradients of temperature and density, making it difficult to determine the localised temperature [95].

Plasma microfields cause the Stark effect, resulting in the broadening of spectral lines. This phenomenon is important in plasma diagnostics, particularly for determining electron density. The Stark contribution to line broadening is typically approximated by a Lorentzian profile, but this approach has significant limitations that affect the accuracy of diagnostics and, consequently, the process control and efficiency of plasma technology applications in the food industry [5]. Lorentzian profiles are associated with homogeneous broadening mechanisms; however, actual profiles may deviate due to lower electron density, ion dynamics, or inhomogeneous microfield distribution. These factors can produce asymmetric broad-wing profiles, and fitting such profiles to a Lorentzian shape can yield electron density values that are systematically higher or lower than the initial estimates. In addition to low electron density and low electron temperature, other line broadening mechanisms can also influence density calculations if they are not negligible compared to Stark broadening. The solution lies in advanced profile modelling that accounts for the influence of ions and microfield distributions, the use of multiple spectral lines for

the simultaneous diagnosis of electron density and temperature, and calibration with independent diagnostics [103,104].

Electron density diagnostics using Stark broadening have not yet become routine in plasma technology applications within the food industry. This need arises from the increasing commercial use of non-thermal plasma, particularly for microbiological inactivation without compromising food quality, as well as for precise control of reactive species that affect processing efficiency. Plasma parameters correlate with the kinetics of processes such as plasma-assisted extractions or texture modifications, making it important to optimise working conditions to achieve the best possible results.

Future development is focused on introducing a metadata schema (MDS) that presents critical parameters in a standardised form, thereby providing information on the operating conditions required to achieve maximum efficiency in plasma technology processes in the food sector [105]. Machine learning models trained on large spectroscopic datasets can assist in interpreting emission spectra and predicting plasma system behaviour, facilitating the optimisation of operating parameters for different food matrices. The standardisation of protocols in plasma diagnostics would enable reproducibility and regulatory acceptance.

7. Comparison of Industrial Applications of OES in Different Plasma Technologies

OES is primarily used in the food sector for elemental analysis, diagnostics plasma used in food processing, and monitoring quality control. OES techniques relevant to the food industry include inductively coupled plasma–OES (ICP-OES), microwave-induced plasma–OES (MIP-OES), dielectric barrier discharge–OES (DBD-OES) and plasma jet–OES (PJ-OES).

OES plays a significant role in food processing assisted by non-thermal plasma, as plasma monitoring and diagnostics are essential for ensuring process repeatability and safety. Measured values of temperature and plasma density confirm operation in a non-thermal regime, which preserves the nutritional and sensory properties of food. Real-time feedback enables the optimisation of operating conditions and adjustment of parameters. Analytical OES, particularly ICP-OES and MIP-OES, is widely used in laboratories for food quality assurance and compliance with food safety regulations, as it allows the simultaneous identification and quantification of multiple elements with high sensitivity in complex food matrices. Although there are numerous applications of OES in various plasma technologies, it has not yet been integrated into industrial practice. Most industrial uses remain limited to laboratory analysis or as a secondary indicator of required information. Increasing food safety standards, especially those related to contamination detection or raw material evaluation, necessitate the introduction of OES into production lines.

The engineering challenges of OES in the context of its application in the food industry cannot be overlooked. OES systems, particularly ICP-OES, require significant financial investment not only in instrumentation but also in specialised infrastructure and trained operators. The interference between complex food matrices and the environment makes real-time application difficult and necessitates sophisticated calibration. The lack of standardisation and the variability of manufacturers' hardware and software packages hinder the integration of OES in the food industry. The application of any OES technique requires qualified personnel with expertise in spectroscopy, plasma physics, and interpretation of the resulting data. Table 12 presents a comparison of industrial applications of OES in different plasma technologies, including detection sensitivities, advantages, limitations, and challenges.

The synergy between plasma processing and optical emission spectroscopy provides a powerful framework for improving food safety control, which has already been recognised. Although not yet integrated into production lines, many commercial food manufacturers

use OES in their in-house analytical laboratories for quality control or in collaboration with scientific research institutions. Despite the limitations and challenges, OES techniques are increasingly being developed for future industrial applications.

Table 12. Comparison of industrial applications of OES in different plasma technologies.

Technique	Applications	Detection Sensitivity	Advantages	Limitations/ Challenges
ICP-OES	Nutritional profiling of food products with multi-element quantification Food quality and authenticity control Food safety assurance with toxic element quantification	µg/L	Simultaneous measurements of multiple elements Low detection limits for many macro-, micro- and trace elements	Sample preparation Sophisticated calibration for matrix interferences Maintenance of complex instrumentation
MIP-OES	Multi-element routine analyses in complex food matrices	µg/L	Comparable performance for many major elements Lower operating costs and simpler infrastructure than ICP-OES	Higher limits of detection for trace elements than ICP-OES
DBD-OES	Cold plasma food decontamination monitoring and control Optimisation of plasma processing Detection of heavy metals in liquid samples	µg/L qualitative	Non-invasive, real-time insights into plasma chemistry relevant to food processing efficacy	Discharge fluctuations in time and space Challenging atmospheric pressure diagnostics Complex spectra overlapping
PJ-OES	Localised surface treatment Monitoring and control of plasma/food surface interaction Optimal parametrisation of plasma processing working conditions	qualitative	Non-invasive, real-time insights into plasma chemistry relevant to food processing efficacy	Small volume samples Strictly controlled working conditions Complicated interpretation of complex emission spectrum

8. Comparison of OES with Alternative Techniques for Food Quality, Authenticity and Safety Monitoring

OES, electrochemical (EC) biosensors, and mass spectrometry (MS) are used as modern alternatives to traditional techniques such as High-Performance Liquid Chromatography (HPLC) and Gas Chromatography (GC) for monitoring food quality, authenticity, and safety.

EC biosensors operate by combining biological recognition elements (enzymes, antibodies, etc.) with electrochemical transducers to convert biological responses into measurable electrical signals (current, voltage, impedance, potential). The advantages of EC sensors include their low cost and portability, making them suitable for online monitoring in industrial environments. Although they provide real-time information, they are usually limited to monitoring surface or bulk properties. When working with complex matrices, contamination or fouling of the electrode surface can occur, reducing data accuracy. The information obtained is an indirect measurement of quantities rather than a direct identification of species, and calibration according to reference standards is mandatory [106–109].

Mass spectrometry is based on the ionisation of molecules from prepared food samples followed by the acceleration of ions in an electric or magnetic field and their separation and detection according to the mass-to-charge ratio. The relative abundance of ions depending on their mass is given in the figure. The main advantage of MS is its very low detection limits, allowing us to detect, identify and quantify not only essential mineral elements but also contaminants in food at extremely low levels, even in trace amounts (parts per billion or

lower). It also aids in determining the geographical origin of food based on specific mineral profiles. The disadvantages are the expensive and technically demanding equipment, the complexity of sample preparation and the provision of high-vacuum conditions, which makes MS an unsuitable technique for monitoring dynamic processes in real time. All limitations lead to the use of MS only in specialised laboratories [110–113].

Techniques such as MS and EC sensors are used to quantify ionic and molecular components after food processing, while OES, in combination with plasma technology, is a technique that enables in situ characterisation of plasma species and the non-invasive monitoring of process dynamics in real time. The creation of reactive species and the monitoring of excited states during food processing using plasma, especially non-thermal plasma, is essential for process control. OES instruments can be integrated into a production line with certain plasma source configurations [114–117]. The advantage of OES compared to MS is the immediate insight into the state of the plasma during processing, and compared to EC sensors, the direct detection of species that trigger chemical changes in food matrices (Table 13).

Table 13. Comparison of EC biosensors, MS and OES.

	Electrochemical Biosensors	Mass Spectrometry	Optical Emission Spectroscopy
Analyte type	Molecules (specific)	Molecules (broad range)	Elements
Quantification	Good (single analyte)	Excellent	Excellent (multi-element)
Sensitivity	Moderate	High	Moderate to high
Portability	High	Low	Low to moderate
Cost	Low	Very high	Moderate to high

9. Conclusions

Plasma technology is widely used in the food industry. The monitoring and control of any method that applies plasma technology require the use of sensors. Invasive sensors (such as electrostatic probes, Langmuir probes, double floating probes, etc.) are placed inside the plasma system. Although they provide data on density, temperature, or flux in the early stages of plasma system development, they also cause perturbations in the produced plasma. Non-invasive sensors (such as OES, ellipsometry, laser-induced fluorescence, etc.) do not affect the dynamics of the plasma system because they do not have direct contact with the plasma, making them ideal for industrial applications. Indirectly collected data require additional analysis to obtain key parameters related to the application of plasma technology. OES, as a non-invasive diagnostic sensor, measures the emission spectra created after the excitation of the sample with the supplied energy. Electrons from excited samples move to higher energy levels, and when they return to lower energy levels they release energy in the form of photons. Each element emits light at precisely defined wavelengths, and OES provides information about the intensity of radiation at particular wavelengths. In addition to its non-destructive effect on the tested sample, OES provides fast and precise identification of elements, even in low concentrations, and enables the real-time monitoring and control of processes. It has been shown that OES can be used to analyse various materials: solids, liquids, and gases. The main plasma parameters, such as temperature and particle number density, can be determined from the obtained emission spectral lines. OES plays a significant role in the quality control of food products by enabling verification of the content of various minerals, including heavy metals. Determining the origin and authenticity of food products (such as olive oil or wine) is simplified using OES. The detection of contaminants in food and beverages using OES ensures the maintenance of food safety in accordance with global safety standards and regulations, and the prevention

or minimisation of potential health risks. All research related to the development of new food products (especially functional foods) or to the improvement of the production process using plasma technology should be accompanied by OES as an advanced and powerful analytical technique.

Author Contributions: Conceptualisation, S.P., E.J., F.M. and N.M.-S.; methodology, S.P. and N.M.-S.; validation, S.P., F.M. and N.M.-S.; investigation, S.P., E.J., F.M. and N.M.-S.; resources, S.P. and N.M.-S.; data curation, S.P., E.J., F.M. and N.M.-S.; writing—original draft preparation, S.P., E.J., F.M. and N.M.-S.; writing—review and editing, S.P., E.J., F.M. and N.M.-S.; visualisation, S.P. and E.J.; supervision, S.P. and N.M.-S.; project administration, S.P. and N.M.-S.; funding acquisition, S.P. and N.M.-S. All authors have read and agreed to the published version of the manuscript.

Funding: This research received no external funding.

Institutional Review Board Statement: Not applicable.

Informed Consent Statement: Not applicable.

Data Availability Statement: Not applicable.

Conflicts of Interest: The authors declare that they have no known competing financial interests or personal relationships that could have appeared to influence the work reported in this paper.

Abbreviations

The following abbreviations are used in this manuscript:

APPJ	Atmospheric pressure plasma jet
CAP	Cold atmospheric plasma
CCD	Charge-coupled device
CP	Cold plasma
DBD	Dielectric barrier discharge
EC	Electrochemical
FWHM	Full Width at Half Maximum
ICP	Inductively coupled plasma
LOD	Limit of detection
LOQ	Limit of quantification
LTE	Local thermodynamic equilibrium
MIP	Microwave-induced plasma
MS	Mass spectrometry
NIST	National Institute of Standards and Technology
NTP	Non-thermal plasma
OES	Optical emission spectroscopy
PJ	Plasma jet
PLTE	Partial local thermodynamic equilibrium
RF	Radio frequency
RNS	Reactive nitrogen species
RONS	Reactive oxygen and nitrogen species
ROS	Reactive oxygen species
UV	Ultraviolet

References

1. Demtröder, W. *Atoms, Molecules and Photons*; Springer: Berlin/Heidelberg, Germany, 2018; ISBN 978-3-662-55521-7. [CrossRef]
2. Mehta, D.; Yadav, S.K. Recent Advances in Cold Plasma Technology for Food Processing. *Food Eng. Rev.* **2022**, *14*, 555–578. [CrossRef]
3. Sasikumar, R.; Selva Kumar, T.; Mangang, I.B.; Kaviarasu, G.; Kaushik, R.; Mansingh, P.; Tomer, V.; Jaiswal, A.K. A Comprehensive Review on Cold Plasma Applications in the Food Industry. *Sustain. Food Technol.* **2025**, *3*, 1251–1274. [CrossRef]

4. Sonawane, S.K.; Marar, T.; Patil, S. Non-Thermal Plasma: An Advanced Technology for Food Industry. *Food Sci. Technol. Int.* **2020**, *26*, 727–740. [CrossRef]
5. Yawut, N.; Mekwilai, T.; Vichiansan, N.; Braspaiboon, S.; Leksakul, K.; Boonyawan, D. Cold Plasma Technology: Trans-forming Food Processing for Safety and Sustainability. *J. Agric. Food Res.* **2024**, *18*, 101383. [CrossRef]
6. Bayati, M.; Lund, M.N.; Tiwari, B.K.; Poojary, M.M. Chemical and Physical Changes Induced by Cold Plasma Treatment of Foods: A Critical Review. *Compr. Rev. Food Sci. Food Saf.* **2024**, *23*, e13376. [CrossRef]
7. Pankaj, S.; Wan, Z.; Keener, K. Effects of Cold Plasma on Food Quality: A Review. *Foods* **2018**, *7*, 4. [CrossRef] [PubMed]
8. Ahmed, M.W.; Gul, K.; Mumtaz, S. Recent Advances in Cold Atmospheric Pressure Plasma for *E. Coli* Decontamination in Food: A Review. *Plasma* **2025**, *8*, 18. [CrossRef]
9. Harikrishna, S.; Anil, P.P.; Shams, R.; Dash, K.K. Cold Plasma as an Emerging Nonthermal Technology for Food Processing: A Comprehensive Review. *J. Agric. Food Res.* **2023**, *14*, 100747. [CrossRef]
10. Punia Bangar, S.; Suri, S.; Nayi, P.; Phimolsiripol, Y. Cold Plasma for Microbial Safety: Principle, Mechanism, and Factors Responsible. *J. Food Process. Preserv.* **2022**, *46*, e16850. [CrossRef]
11. Farooq, S.; Dar, A.H.; Dash, K.K.; Srivastava, S.; Pandey, V.K.; Ayoub, W.S.; Pandiselvam, R.; Manzoor, S.; Kaur, M. Cold Plasma Treatment Advancements in Food Processing and Impact on the Physiochemical Characteristics of Food Products. *Food Sci. Biotechnol.* **2023**, *32*, 621–638. [CrossRef] [PubMed]
12. Katsigiannis, A.S.; Bayliss, D.L.; Walsh, J.L. Cold Plasma for the Disinfection of Industrial Food-contact Surfaces: An Overview of Current Status and Opportunities. *Compr. Rev. Food Sci. Food Saf.* **2022**, *21*, 1086–1124. [CrossRef]
13. Kauser, S.; Hussain, A.; Imtiaz, S.; Murtaza, M.A.; Ali, M.Q.; Najam, A.; Ashfaq, M.; Firdous, N.; Zia, M.; Bakhtawar, F.; et al. Cold Plasma Technology: An Epochal Enabler in Elevating Food Preservation, Ensuring Safety, and Enhancing Quality Standards. *Discov. Appl. Sci.* **2025**, *7*, 625. [CrossRef]
14. Ding, T.; Cullen, P.J.; Yan, W. (Eds.) *Applications of Cold Plasma in Food Safety*; Springer: Singapore, 2022; ISBN 978-981-16-1826-0. [CrossRef]
15. Amjad, N.; Karabulut, G.; Wei, C.R.; Naseer, M.S.; Imran, A.; Chauhan, A.; Islam, F.; Biswas, S. A Review on Cold Plasma Technology for Pesticide-Free Food Safety: Mechanisms, Efficiency, and Future Perspectives. *Curr. Res. Nutr. Food Sci.* **2025**, *13*, 569–583. [CrossRef]
16. Nwabor, O.F.; Onyeaka, H.; Miri, T.; Obileke, K.; Anumudu, C.; Hart, A. A Cold Plasma Technology for Ensuring the Microbiological Safety and Quality of Foods. *Food Eng. Rev.* **2022**, *14*, 535–554. [CrossRef]
17. Mishra, A.; Mishra, R.; Siddiqui, Y.H.; Jangra, S.; Pandey, S.; Prakash, R. Analysis of Discharge Parameters of an Argon Cold Atmospheric Pressure Plasma Jet and Its Impact on Surface Characteristics of White Grapes. *Phys. Scr.* **2024**, *99*, 105615. [CrossRef]
18. Šrámková, P.; Kostoláni, D.; Kyzek, S.; Bathoova, M.; Ďurčányová, S.; Stupavská, M.; Gálová, E.; Zahoranová, A.; Švubová, R. Extending Shelf Life: Cold Plasma as a Tool to Preserve Long-Term Germination Potential of Pea Seeds. *Sci. Rep.* **2025**, *15*, 35001. [CrossRef] [PubMed]
19. Ucar, Y.; Ceylan, Z.; Durmus, M.; Tomar, O.; Cetinkaya, T. Application of Cold Plasma Technology in the Food Industry and Its Combination with Other Emerging Technologies. *Trends Food Sci. Technol.* **2021**, *114*, 355–371. [CrossRef]
20. Laroque, D.A.; Seó, S.T.; Valencia, G.A.; Laurindo, J.B.; Carciofi, B.A.M. Cold Plasma in Food Processing: Design, Mechanisms, and Application. *J. Food Eng.* **2022**, *312*, 110748. [CrossRef]
21. Shill, N.; Sit, N. Application of Cold Plasma as a Technique for Minimal Processing of Fruits. *Food Prod. Process. Nutr.* **2025**, *7*, 43. [CrossRef]
22. Usman, I.; Afzaal, M.; Imran, A.; Saeed, F.; Afzal, A.; Ashfaq, I.; Shah, Y.A.; Islam, F.; Azam, I.; Tariq, I.; et al. Recent Updates and Perspectives of Plasma in Food Processing: A Review. *Int. J. Food Prop.* **2023**, *26*, 552–566. [CrossRef]
23. Park, S.; Choe, W.; Moon, S.Y.; Yoo, S.J. Electron Characterization in Weakly Ionized Collisional Plasmas: From Principles to Techniques. *Adv. Phys. X* **2019**, *4*, 1526114. [CrossRef]
24. Fujimoto, T. Plasma Spectroscopy. In *Plasma Polarization Spectroscopy*; Springer: Berlin/Heidelberg, Germany, 2008; pp. 29–49. [CrossRef]
25. Herman, I.P. Optical Emission Spectroscopy. In *Optical Diagnostics for Thin Film Processing*; Elsevier: Amsterdam, The Netherlands, 1996; pp. 157–213. [CrossRef]
26. Kunze, H.-J. *Introduction to Plasma Spectroscopy*; Springer: Berlin/Heidelberg, Germany, 2009; Volume 56, ISBN 978-3-642-02232-6. [CrossRef]
27. Fantz, U. Basics of Plasma Spectroscopy. *Plasma Sources Sci. Technol.* **2006**, *15*, S137–S147. [CrossRef]
28. Ochkin, V.N. *Spectroscopy of Low Temperature Plasma*; Wiley: Weinheim, Germany, 2009; ISBN 9783527407781. [CrossRef]
29. Thirumdas, R.; Janve, M.; Siliveru, K.; Kothakota, A. Determination of Food Quality Using Atomic Emission Spectroscopy. In *Evaluation Technologies for Food Quality*; Elsevier: Amsterdam, The Netherlands, 2019; pp. 175–192. [CrossRef]
30. Zaplotnik, R.; Primc, G.; Vesel, A. Optical Emission Spectroscopy as a Diagnostic Tool for Characterization of Atmospheric Plasma Jets. *Appl. Sci.* **2021**, *11*, 2275. [CrossRef]

31. Khan, S.R.; Sharma, B.; Chawla, P.A.; Bhatia, R. Inductively Coupled Plasma Optical Emission Spectrometry (ICP-OES): A Powerful Analytical Technique for Elemental Analysis. *Food Anal. Methods* **2022**, *15*, 666–688. [CrossRef]
32. Kakuk, M.; Farkas, D.; Kállai-Szabó, B.; Pencz, K.; Mészáros, L.A.; Tonka-Nagy, P.G.; Kállai-Szabó, N.; Antal, I. Inductively Coupled Plasma Optical Emission Spectroscopy (ICP-OES): Exploring Versatile Applications in Industrial and Analytical Fields. *Period. Polytech. Chem. Eng.* **2025**, *69*, 339–360. [CrossRef]
33. Hanna, A.R.; Fisher, E.R. Investigating Recent Developments and Applications of Optical Plasma Spectroscopy: A Review. *J. Vac. Sci. Technol. A Vac. Surf. Films* **2020**, *38*, 020806. [CrossRef]
34. Yeung, V.; Miller, D.D.; Rutzke, M.A. Atomic Absorption Spectroscopy, Atomic Emission Spectroscopy, and Inductively Coupled Plasma-Mass Spectrometry. In *Food Analysis*; Food Science Text Series; Nielsen, S.S., Ed.; Springer: Cham, Switzerland, 2017; pp. 129–150. [CrossRef]
35. Hou, X.; Amais, R.S.; Jones, B.T.; Donati, G.L. Inductively Coupled Plasma Optical Emission Spectrometry. In *Encyclopedia of Analytical Chemistry*; Wiley: Hoboken, NJ, USA, 2021; pp. 1–25. [CrossRef]
36. Senila, M. Recent Advances in the Determination of Major and Trace Elements in Plants Using Inductively Coupled Plasma Optical Emission Spectrometry. *Molecules* **2024**, *29*, 3169. [CrossRef] [PubMed]
37. Senila, M.; Cadar, O. Determination of Metals in Wine by ICP-OES: Comparative Study of Matrix Effects and Greenness of Different Sample Preparation Approaches. *J. Food Compos. Anal.* **2025**, *148*, 108331. [CrossRef]
38. Douvris, C.; Vaughan, T.; Bussan, D.; Bartzas, G.; Thomas, R. How ICP-OES Changed the Face of Trace Element Analysis: Review of the Global Application Landscape. *Sci. Total Environ.* **2023**, *905*, 167242. [CrossRef]
39. Liu, H.; Meng, Q.; Zhao, X.; Ye, Y.; Tong, H. Inductively Coupled Plasma Mass Spectrometry (ICP-MS) and Inductively Coupled Plasma Optical Emission Spectrometer (ICP-OES)-Based Discrimination for the Authentication of Tea. *Food Control* **2021**, *123*, 107735. [CrossRef]
40. Di Donato, F.; Biancolillo, A.; Foschi, M.; Di Cecco, V.; Di Martino, L.; D'Archivio, A.A. Authentication of Typical Italian Bell Pepper Spices by ICP-OES Multi-Elemental Analysis Combined with SIMCA Class Modelling. *J. Food Compost. Anal.* **2023**, *115*, 104948. [CrossRef]
41. Bhalodia, A.; Desai, S. Comprehensive Assessment of Greenness of ICP-OES Methods for Determination of Metals. *Green Anal. Chem.* **2025**, *12*, 100222. [CrossRef]
42. Elghnam, S.M.; Aborhyem, S.M.; Khedr, Y.I. Manganese Quantification in Some Egyptian Food Items Using Inductively Coupled Plasma Optical Emission Spectroscopy. *CYTA J. Food* **2022**, *20*, 199–205. [CrossRef]
43. Koch, W.; Czop, M.; Nawrocka, A.; Wiącek, D. Contribution of Major Groups of Food Products to the Daily Intake of Se-lected Elements—Results from Analytical Determinations Supported by Chemometric Analysis. *Nutrients* **2020**, *12*, 3412. [CrossRef]
44. Nascimento, A.C.; Motta, C.; Rego, A.; Delgado, I.; Santiago, S.; Assunção, R.; Matos, A.S.; Santos, M.; Castanheira, I. Measuring Minerals in Pseudocereals Using Inductively Coupled Plasma Optical Emission Spectrometry: What Is the Op-timal Digestion Method? *Foods* **2025**, *14*, 565. [CrossRef] [PubMed]
45. Pastor, K.; Nastić, N.; Ilić, M.; Skendi, A.; Stefanou, S.; Ačanski, M.; Rocha, J.M.; Papageorgiou, M. A Screening Study of Elemental Composition in Legume (*Fabaceae* sp.) Cultivar from Serbia: Nutrient Accumulation and Risk Assessment. *J. Food Compost. Anal.* **2024**, *130*, 106127. [CrossRef]
46. Koch, W.; Czop, M.; Iłowiecka, K.; Nawrocka, A.; Wiącek, D. Dietary Intake of Toxic Heavy Metals with Major Groups of Food Products—Results of Analytical Determinations. *Nutrients* **2022**, *14*, 1626. [CrossRef]
47. Louppis, A.P.; Karabagias, I.K.; Papastephanou, C.; Badeka, A. Two-Way Characterization of Beekeepers' Honey According to Botanical Origin on the Basis of Mineral Content Analysis Using ICP-OES Implemented with Multiple Chemometric Tools. *Foods* **2019**, *8*, 210. [CrossRef] [PubMed]
48. Manousi, N.; Isaakidou, E.; Zachariadis, G.A. An Inductively Coupled Plasma Optical Emission Spectrometric Method for the Determination of Toxic and Nutrient Metals in Spices after Pressure-Assisted Digestion. *Appl. Sci.* **2022**, *12*, 534. [CrossRef]
49. Fermo, P.; Comite, V.; Sredojević, M.; Ćirić, I.; Gašić, U.; Mutić, J.; Baošić, R.; Tešić, Ž. Elemental Analysis and Phenolic Profiles of Selected Italian Wines. *Foods* **2021**, *10*, 158. [CrossRef]
50. Mphande, J.; Chishimba, S.; Kabwe, J.; Mwamba, F.K.; Taimolo, L.; Mutale, B.; Simutenda, J.; Nkweto, E.; Simfukwe, K.; Muchimba, J.; et al. Heavy and Trace Metals in Zambian Honey: Are Consumers at Risk? *Cogent Food Agric.* **2026**, *12*, 2609356. [CrossRef]
51. Fernandes Júnior, S.L.; Gonçalves, P.M.; Batista, D.B.; Luna, A.S.; Ferreira, F.N.; Pinto, L.; de Gois, J.S. Banana Flour Adulteration Key Marker Unravelled by Inductively Coupled Plasma Optical Emission Spectrometry Assisted by Chemometric Tools. *Chemosensors* **2025**, *13*, 153. [CrossRef]
52. Silva, A.F.S.; Martins, L.C.; Moraes, L.M.B.; Gonçalves, I.C.; de Godoy, B.B.R.; Erasmus, S.W.; van Ruth, S.; Rocha, F.R.P. Can Minerals Be Used as a Tool to Classify Cinnamon Samples? In *Proceedings of the 1st International Electronic Conference on Food Science and Functional Foods*; MDPI: Basel, Switzerland, 2020; p. 22.

53. Phan-Thien, K.-Y.; Wright, G.C.; Lee, N.A. Inductively Coupled Plasma-Mass Spectrometry (ICP-MS) and -Optical Emission Spectroscopy (ICP–OES) for Determination of Essential Minerals in Closed Acid Digestates of Peanuts (*Arachis hypogaea* L.). *Food Chem.* **2012**, *134*, 453–460. [CrossRef]
54. Huang, M.; Li, X. Quantitative Detection of Toxic Elements in Food Samples by Inductively Coupled Plasma Mass Spectrometry (ICP-MS). *Processes* **2025**, *13*, 3361. [CrossRef]
55. Szymczycha-Madeja, A. Rapid Method of Element Determination in Rye Crispbread by ICP OES. *Arab. J. Chem.* **2017**, *10*, S3913–S3919. [CrossRef]
56. Ngigi, A.N.; Muraguri, B.M. ICP-OES Determination of Essential and Non-Essential Elements in Moringa Oleifera, Salvia Hispanica and Linum Usitatissimum. *Sci. Afr.* **2019**, *6*, e00165. [CrossRef]
57. Liu, S.; Yang, D.; Huang, J.; Huang, H.; Sun, J.; Yang, Z.; Zhou, C. Advances in Atmospheric Cold Plasma Technology for Plant-Based Food Safety, Functionality, and Quality Implications. *Foods* **2025**, *14*, 2999. [CrossRef]
58. Ozbek, N.; Koca, M.; Akman, S. A Practical Method for the Determination of Al, B, Co, Cr, Cu, Fe, Mg, Mn, Pb, and Zn in Different Types of Vinegars by Microwave Induced Plasma Optical Emission Spectrometry. *Food Anal. Methods* **2016**, *9*, 2246–2250. [CrossRef]
59. São Bernardo Carvalho, L.; Santos Silva, C.; Araújo Nóbrega, J.; Santos Boa Morte, E.; Muniz Batista Santos, D.C.; Andrade Korn, M.G. Microwave Induced Plasma Optical Emission Spectrometry for Multielement Determination in Instant Soups. *J. Food Compos. Anal.* **2020**, *86*, 103376. [CrossRef]
60. da Silva, E.S.; Freitas, J.M.; Brandão, J.P.C.; Simões, I.F.; Lenz, A.R.; Drewinski, M.D.P.; Morais, Á.C.; Menolli, N.; de Freitas Santos, A. Multi-Element Determination in Wild and Cultivated Edible Mushrooms from the Brazilian Atlantic Forest Using Microwave-Induced Plasma Optical Emission Spectrometry (MIP OES). *Analytica* **2025**, *6*, 21. [CrossRef]
61. Iaquinta, F.; Mollo, A.; Machado, I.; Vögler, R.; Banhos, S.G.; Nogueira, A.R.A. Microwave-Induced Plasma Optical Emis-sion Spectrometry Coupled to Vapor Generation (VG-MIP OES) as an Alternative Technique for As and Hg Determination for Seafood Surveillance. *Spectrochim. Acta Part B At. Spectrosc.* **2025**, *232*, 107281. [CrossRef]
62. Oliveira, L.B.; de Melo, J.C.; da Boa Morte, E.S.; de Jesus, R.M.; Teixeira, L.S.G.; Korn, M.G.A. Multi-Element Determination in Chocolate Bars by Microwave-Induced Plasma Optical Emission Spectrometry. *Food Chem.* **2021**, *351*, 129285. [CrossRef]
63. Braden, J.L.; Klarquist, E.F.; Kellogg, J.A. Determination of Elements in Cereals, Pseudocereals, and Legumes by Microwave Plasma-Atomic Emission Spectrometry. *Food Chem. X* **2024**, *24*, 101844. [CrossRef] [PubMed]
64. Müller, A.; Pozebon, D.; Dressler, V.L. Advances of Nitrogen Microwave Plasma for Optical Emission Spectrometry and Applications in Elemental Analysis: A Review. *J. Anal. At. Spectrom.* **2020**, *35*, 2113–2131. [CrossRef]
65. Wiltsche, H.; Wolfgang, M. Merits of Microwave Plasmas for Optical Emission Spectrometry—Characterization of an Axially Viewed Microwave-Sustained, Inductively Coupled, Atmospheric-Pressure Plasma (MICAP). *J. Anal. At. Spectrom.* **2020**, *35*, 2369–2377. [CrossRef]
66. Sojithamporn, P.; Leksakul, K.; Sawangrat, C.; Charoenchai, N.; Boonyawan, D. Degradation of Pesticide Residues in Water, Soil, and Food Products via Cold Plasma Technology. *Foods* **2023**, *12*, 4386. [CrossRef] [PubMed]
67. Li, B.; Peng, L.; Cao, Y.; Liu, S.; Zhu, Y.; Dou, J.; Yang, Z.; Zhou, C. Insights into Cold Plasma Treatment on the Cereal and Legume Proteins Modification: Principle, Mechanism, and Application. *Foods* **2024**, *13*, 1522. [CrossRef]
68. Dharini, M.; Jaspin, S.; Mahendran, R. Cold Plasma Reactive Species: Generation, Properties, and Interaction with Food Biomolecules. *Food Chem.* **2023**, *405*, 134746. [CrossRef]
69. Figueroa-Pinochet, M.F.; Castro-Alija, M.J.; Tiwari, B.K.; Jiménez, J.M.; López-Vallecillo, M.; Cao, M.J.; Albertos, I. Dielectric Barrier Discharge for Solid Food Applications. *Nutrients* **2022**, *14*, 4653. [CrossRef] [PubMed]
70. Kiš, M.; Milošević, S.; Vulić, A.; Herceg, Z.; Vukušić, T.; Pleadin, J. Efficacy of Low Pressure DBD Plasma in the Reduction of T-2 and HT-2 Toxin in Oat Flour. *Food Chem.* **2020**, *316*, 126372. [CrossRef]
71. Zheng, Z.; Huang, Y.; Liu, L.; Chen, Y.; Wang, Y.; Li, C. Zearalenone Degradation by Dielectric Barrier Discharge Cold Plasma: The Kinetics and Mechanism. *Foods* **2022**, *11*, 1494. [CrossRef] [PubMed]
72. Kumar Mahnot, N.; Siyu, L.-P.; Wan, Z.; Keener, K.M.; Misra, N.N. In-Package Cold Plasma Decontamination of Fresh-Cut Carrots: Microbial and Quality Aspects. *J. Phys. D Appl. Phys.* **2020**, *53*, 154002. [CrossRef]
73. Cai, Y.; Gao, X.-G.; Ji, Z.-N.; Yu, Y.-L.; Wang, J.-H. Nonthermal Optical Emission Spectrometry for Simultaneous and Direct Determination of Zinc, Cadmium and Mercury in Spray. *Analyst* **2018**, *143*, 930–935. [CrossRef]
74. Qian, B.; Zhao, J.; He, Y.; Peng, L.; Ge, H.; Han, B. Miniaturized Dielectric Barrier Discharge-Molecular Emission Spec-trometer for Determination of Total Sulfur Dioxide in Food. *Food Chem.* **2020**, *317*, 126437. [CrossRef]
75. Wang, X.-S.; Wang, Y.; Wu, C.-X.; Shu, Y.; Wei, X.; Chen, M.-L.; Wang, J.-H. Dielectric Barrier Discharge Atomic Emission Spectrometry Coupled with Cryogenic Sampling for Rapid Element Imaging. *Microchem. J.* **2025**, *219*, 115846. [CrossRef]
76. Zhang, D.-J.; Cai, Y.; Chen, M.-L.; Yu, Y.-L.; Wang, J.-H. Dielectric Barrier Discharge-Optical Emission Spectrometry for the Simultaneous Determination of Halogens. *J. Anal. At. Spectrom.* **2016**, *31*, 398–405. [CrossRef]

77. Cyganowski, P.; Terefinko, D.; Motyka-Pomagruk, A.; Babinska-Wensierska, W.; Khan, M.A.; Klis, T.; Sledz, W.; Lojkowska, E.; Jamroz, P.; Pohl, P.; et al. The Potential of Cold Atmospheric Pressure Plasmas for the Direct Degradation of Organic Pollutants Derived from the Food Production Industry. *Molecules* **2024**, *29*, 2910. [CrossRef] [PubMed]
78. Huang, J.; Zhou, C.; Huang, H.; Yang, Z.; Liu, S. Cold Plasma as a Promising Non-Thermal Strategy for Enhancing Food Safety: A Review of Microbial and Mycotoxin Decontamination. *Molecules* **2026**, *31*, 517. [CrossRef] [PubMed]
79. Rout, S.; Panda, P.K.; Dash, P.; Srivastav, P.P.; Hsieh, C.-T. Cold Plasma-Induced Modulation of Protein and Lipid Mac-romolecules: A Review. *Int. J. Mol. Sci.* **2025**, *26*, 1564. [CrossRef]
80. Zhou, Y.; Zuo, H.; Dai, Z.; Guo, Z.; Holman, B.W.B.; Ding, Y.; Shi, J.; Ding, X.; Huang, M.; Mao, Y. Changes to Pork Bacterial Counts and Composition After Dielectric Barrier Discharge Plasma Treatment and Storage in Modified-Atmosphere Packaging. *Foods* **2024**, *13*, 4162. [CrossRef]
81. Atani, S.H.; Soltanizadeh, N.; Shahedi, M.; Ghomi, H. The Potential of Atmospheric Dielectric Barrier Discharge (DBD) Plasma Method for Beef Thawing. *Future Foods* **2025**, *11*, 100600. [CrossRef]
82. Thana, P.; Boonyawan, D.; Jaikua, M.; Promsart, W.; Rueangwong, A.; Ungwiwatkul, S.; Prasertboonyai, K.; Maitip, J. Plasma-Activated Water (PAW) Decontamination of Foodborne Bacteria in Shucked Oyster Meats Using a Compact Flow-Through Generator. *Foods* **2025**, *14*, 1502. [CrossRef]
83. Dousti, M.; Bashiry, M.; Zohrabi, P.; Siahpoush, V.; Ghaani, A.; Abdolmaleki, K. The Effect of Dielectric Barrier Discharge (DBD) Cold Plasma Treatment on the Reduction of Aflatoxin B1 and the Physicochemical Properties of Oat. *Appl. Food Res.* **2024**, *4*, 100515. [CrossRef]
84. Leandro, G.C.; Laroque, D.A.; Monteiro, A.R.; Carciofi, B.A.M.; Valencia, G.A. Current Status and Perspectives of Starch Powders Modified by Cold Plasma: A Review. *J. Polym. Environ.* **2024**, *32*, 510–523. [CrossRef]
85. Burducea, I.; Burducea, C.; Mereuta, P.-E.; Sirbu, S.-R.; Iancu, D.-A.; Istrati, M.-B.; Straticiuc, M.; Lungoci, C.; Stoleru, V.; Teliban, G.-C.; et al. Helium Atmospheric Pressure Plasma Jet Effects on Two Cultivars of *Triticum aestivum* L. *Foods* **2023**, *12*, 208. [CrossRef]
86. Chen, M.; Wang, C.; Xie, T.; Chen, Z.; Xu, G. Inactivation Effect and Influencing Factors of Cold Atmospheric Plasma Treatment with Bacteria on Food Contact Materials. *Plasma* **2025**, *8*, 46. [CrossRef]
87. Orlowski, J.; Motyka-Pomagruk, A.; Dzimitrowicz, A.; Pohl, P.; Terefinko, D.; Lojkowska, E.; Jamroz, P.; Sledz, W. Appli-cation of Cold Atmospheric Pressure Plasma Jet Results in Achievement of Universal Antibacterial Properties on Various Plant Seeds. *Appl. Sci.* **2025**, *15*, 1255. [CrossRef]
88. Svarnas, P.; Poupouzas, M.; Papalexopoulou, K.; Kalaitzopoulou, E.; Skipitari, M.; Papadea, P.; Varemmenou, A.; Gianna-kopoulos, E.; Georgiou, C.D.; Georga, S.; et al. Water Modification by Cold Plasma Jet with Respect to Physical and Chemical Properties. *Appl. Sci.* **2022**, *12*, 11950. [CrossRef]
89. Förster, S.; Mohr, C.; Viöl, W. Investigations of an Atmospheric Pressure Plasma Jet by Optical Emission Spectroscopy. *Surf. Coat. Technol.* **2005**, *200*, 827–830. [CrossRef]
90. Giannakaris, N.; Niebauer, M.; Gürtler, G.; Kleŝtinec, R.; Pořízka, P.; Kaiser, J.; Stehrer, T.; Pedarnig, J.D. Surface Cleaning with Atmospheric Pressure Plasma Jet Investigated by In-Situ Optical Emission Spectroscopy and Laser-Induced Break-down Spectroscopy. *Appl. Surf. Sci.* **2025**, *684*, 161751. [CrossRef]
91. Kosumsupamala, K.; Thana, P.; Palee, N.; Lamasai, K.; Kuensaen, C.; Ngamjarurojana, A.; Yangkhamman, P.; Boonyawan, D. Air to H2-N2 Pulse Plasma Jet for In-Vitro Plant Tissue Culture Process: Source Characteristics. *Plasma Chem. Plasma Process.* **2022**, *42*, 535–559. [CrossRef]
92. Tanakaran, Y.; Matra, K. The Influence of Atmospheric Non-Thermal Plasma on Jasmine Rice Seed Enhancements. *J. Plant Growth Regul.* **2022**, *41*, 178–187. [CrossRef]
93. Ullah, N.; Khan, M.I.; Qamar, A.; Rehman, N.-U.; Tag elDin, E.; Alkhedher, M.; Majid, A. Metrology of Ar–N_2/O_2 Mixture Atmospheric Pressure Pulsed DC Jet Plasma and Its Application in Bio-Decontamination. *ACS Omega* **2023**, *8*, 12028–12038. [CrossRef]
94. Fridman, A.A. *Plasma Chemistry*; Cambridge University Press: Cambridge, UK, 2008; ISBN 978-0-521-84735-3.
95. Akatsuka, H. Optical Emission Spectroscopic (OES) Analysis for Diagnostics of Electron Density and Temperature in Non-Equilibrium Argon Plasma Based on Collisional-Radiative Model. *Adv. Phys. X* **2019**, *4*, 1592707. [CrossRef]
96. NIST (National Institute of Standards and Technology). NIST Atomic Spectra Database (Ver. 5.12). Available online: https://physics.nist.gov/asd (accessed on 15 December 2025).
97. Gigosos, M.A. Stark Broadening Models for Plasma Diagnostics. *J. Phys. D Appl. Phys.* **2014**, *47*, 343001. [CrossRef]
98. Thouin, J.; Benmouffok, M.; Freton, P.; Gonzalez, J.-J. Interpretation of Stark Broadening Measurements on a Spatially Integrated Plasma Spectral Line. *EPJ Appl. Phys.* **2022**, *97*, 87. [CrossRef]
99. Konjević, N.; Lesage, A.; Fuhr, J.R.; Wiese, W.L. Experimental Stark Widths and Shifts for Spectral Lines of Neutral and Ionized Atoms (A Critical Review of Selected Data for the Period 1989 Through 2000). *J. Phys. Chem. Ref. Data* **2002**, *31*, 819–927. [CrossRef]

100. Ahmed, N.; Masood, A.; Mumtaz, R.; Wee, M.F.M.R.; Chan, K.M.; Patra, A.; Siow, K.S. Quad-Atmospheric Pressure Plasma Jet (q-APPJ) Treatment of Chilli Seeds to Stimulate Germination. *Plasma Chem. Plasma Process.* **2024**, *44*, 509–522. [CrossRef]
101. Chalise, R.; Dhungana, S.; Sharma, S.; Basnet, S.; Baniya, H.B.; Acharya, T.R.; Lamichhane, P.; Khanal, R. Development and Characterization of Atmospheric Pressure Gliding Arc Plasma Jet. *Phys. Scr.* **2024**, *99*, 105611. [CrossRef]
102. Pleslić, S.; Katalenić, F. Monitoring and Diagnostics of Non-Thermal Plasmas in the Food Sector Using Optical Emission Spectroscopy. *Appl. Sci.* **2025**, *15*, 8325. [CrossRef]
103. Palomares, J.M.; Hübner, S.; Carbone, E.A.D.; de Vries, N.; van Veldhuizen, E.M.; Sola, A.; Gamero, A.; van der Mullen, J.J.A.M. Hβ Stark Broadening in Cold Plasmas with Low Electron Densities Calibrated with Thomson Scattering. *Spectrochim. Acta Part B At. Spectrosc.* **2012**, *73*, 39–47. [CrossRef]
104. Yubero, C.; García, M.C.; Dimitrijevic, M.S.; Sola, A.; Gamero, A. Measuring the Electron Density in Plasmas from the Difference of Lorentzian Part of the Widths of Two Balmer Series Hydrogen Lines. *Spectrochim. Acta Part B At. Spectrosc.* **2015**, *107*, 164–169. [CrossRef]
105. Pampoukis, G.; Weihe, T.; Wagner, R.; Becker, M.M.; Yao, Y.; Nierop Groot, M.N.; Schnabel, U. A Metadata Schema to Standardize Non-Thermal Plasma Decontamination Parameters in Food-Related Applications. *Sci. Data* **2025**, *12*, 838. [CrossRef]
106. Brunetti, B. Electrochemical Sensors and Biosensors for the Determination of Food Nutritional and Bioactive Compounds: Recent Advances. *Sensors* **2024**, *24*, 6588. [CrossRef] [PubMed]
107. Hosseinikebria, S.; Khazaei, M.; Dervisevic, M.; Judicpa, M.A.; Tian, J.; Razal, J.M.; Voelcker, N.H.; Nilghaz, A. Electro-chemical Biosensors: The Beacon for Food Safety and Quality. *Food Chem.* **2025**, *475*, 143284. [CrossRef]
108. Kumar, A.; Kulshreshtha, S.; Shrivastava, A.; Saini, A. Biosensors for Food Spoilage Detection: A Comprehensive Review of Current Advances. *J. Food Chem. Nanotechnol.* **2024**, *10*, S73–S82. [CrossRef]
109. Wu, X.; Yuan, Z.; Gao, S.; Zhang, X.; El-Mesery, H.S.; Lu, W.; Dai, X.; Xu, R. Electrochemical Biosensors Driving Model Transformation for Food Testing. *Foods* **2025**, *14*, 2669. [CrossRef]
110. Núñez, N.; Lucci, P.; Núñez, O. *Mass Spectrometry in Food Analysis*; World Scientific: Singapore, 2025; ISBN 978-981-12-9623-9. [CrossRef]
111. Tortorella, S.; Bartels, B.; Suman, M.; Heeren, R.M.A.; Righetti, L. Mass Spectrometry Imaging in Food Safety and Authen-ticity: Overcoming Challenges and Exploring Opportunities. *Trends Food Sci. Technol.* **2025**, *155*, 104803. [CrossRef]
112. Wang, Y.; Gao, S.; Wu, J.; Li, X.; Zhao, Y.; Zhou, L.; Hua, Y.; Kang, L.; Qiu, Z. Non-Destructive Food Authentication by Vapor-Assisted Desorption Chemical Ionization Mass Spectrometry Paired with Machine Learning. *NPJ Sci. Food* **2025**, *9*, 271. [CrossRef] [PubMed]
113. Witjaksono, G.; Alva, S. Applications of Mass Spectrometry to the Analysis of Adulterated Food. In *Mass Spectrometry—Future Perceptions and Applications*; IntechOpen: London, UK, 2019. [CrossRef]
114. Hadian, Z.; Shariatifar, N.; Arabameri, M.; Moazzen, M.; Mousavi Khaneghah, A. Risk Assessment of Metal Exposure from Nuts Consumption in Iran Using Inductively Coupled Plasma Optical Emission Spectroscopy (ICP-OES). *J. Agric. Food Res.* **2025**, *21*, 101865. [CrossRef]
115. Pérez-Vázquez, J.; García-Juan, A.; Serrano, R.; Grindlay, G.; Gras, L. Direct Multi-Elemental Analysis of Wines by Means of Microwave-Sustained Inductively Coupled Atmospheric-Pressure Plasma Optical Emission Spectroscopy (MICAP-OES). *Microchem. J.* **2025**, *213*, 113655. [CrossRef]
116. Takagi, H.; Sakamoto, N.; Shibuta, Y.; Yamashita, M. Mercury Monitoring in Farmed Pacific Bluefin Tuna (Thunnus Ori-entalis) Using Liquid Asymmetric-Electrode Plasma Optical Emission Spectroscopy: Ventricle Tissue as a Potential Indicator. *Food Control* **2025**, *169*, 110997. [CrossRef]
117. Zuma, M.C.; Mdluli, N.S.; Sihlahla, M.; Mketo, N. Determination of Essential and Non-Essential Elements of Commercialized Rooibos Tea Samples Using Microwave-Assisted Digestion Prior to Analysis Using Inductively Coupled Plasma-Optical Emission Spectroscopy: Human Health Risk Assessments. *Food Chem. Adv.* **2025**, *9*, 101161. [CrossRef]